PNAS, Research Article

Section: *Biochemistry*

October 8, 2020

Supporting Information (SI):

The Arg/N-degron pathway targets transcription factors and regulates specific genes

Tri T. M. Vu[a], Dylan C. Mitchell[b], Steven P. Gygi[b] and Alexander Varshavsky[a,1]

[a]Division of Biology and Biological Engineering,
California Institute of Technology, Pasadena, CA 91125, USA

[b]Department of Cell Biology, Harvard Medical School, Boston, MA 02115

[1]Track-III paper, contributed by Alexander Varshavsky.

Email: avarsh@caltech.edu. Telephone: 818-606-1908.

Running title: Regulation by the Arg/N-degron pathway

Keywords: transcription, degradation, UBR1, GR, PREP1.

This PDF contains:

Figures S1-S13 and their legends.

Materials and Methods.

Tables S1 and S2.

References for SI.

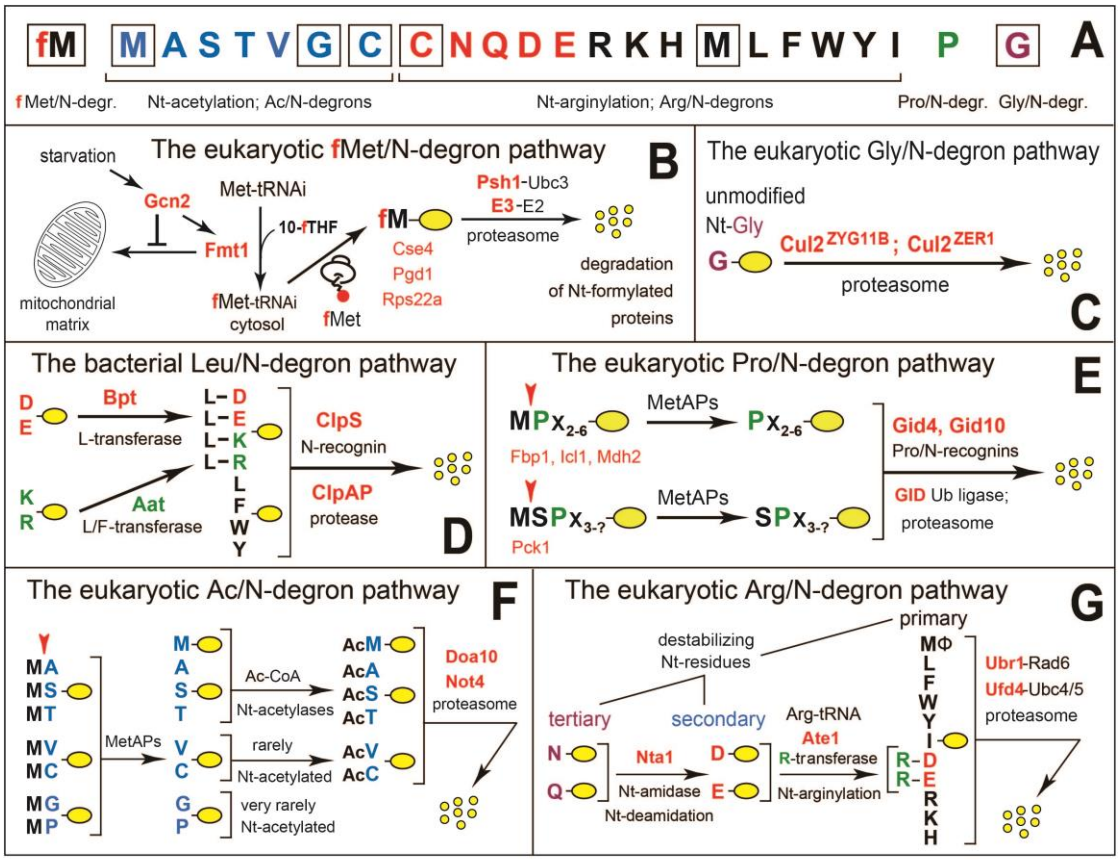

Fig. S1. N-degron pathways. N-terminal (Nt) residues are indicated by single-letter abbreviations. A yellow oval denotes the rest of a protein substrate. (*A*) Twenty amino acids of the genetic code are arranged to delineate Nt-residues of N-degrons. Amino acids that are cited more than once are marked by square frames. Nt-Met is cited thrice, since it can be recognized by the Ac/N-degron pathway, as Nt-acetylated Ac-Met, by the Arg/N-degron pathway, as unacetylated Nt-Met, and by the fMet/N-degron pathway, as Nt-formylated fMet. Nt-Cys is cited twice, since it can be recognized by the Ac/N-degron pathway, as Nt-acetylated Cys, and by the Arg/N-degron pathway, as Nt-arginylatable Nt-Cys sulfinate or Nt-Cys-sulfonate, formed in multicellular eukaryotes but apparently not in unstressed *S. cerevisiae*. Nt-Gly is cited twice, since it can be recognized by the Gly/N-degron pathway, as unmodified Mt-Gly, and by the Ac/N-degron pathway, as (rarely) Nt-acetylated Gly. (*B*) The eukaryotic (*Saccharomyces cerevisiae*) fMet/N-degron pathway. 10-fTHF, 10-formyltetrahydrofolate. (*C*) The eukaryotic (mammalian) Gly/N-degron pathway. (*D*) The bacterial (*Vibrio vulnificus*) Leu/N-degron pathway. (*E*) The eukaryotic (*S. cerevisiae*) Pro/N-degron pathway. (*F*) The eukaryotic (*S. cerevisiae*) Ac/N-degron pathway. (G*)* The eukaryotic (*S. cerevisiae*) Arg/N-degron pathway. See the main text (Introduction) for references and other details.

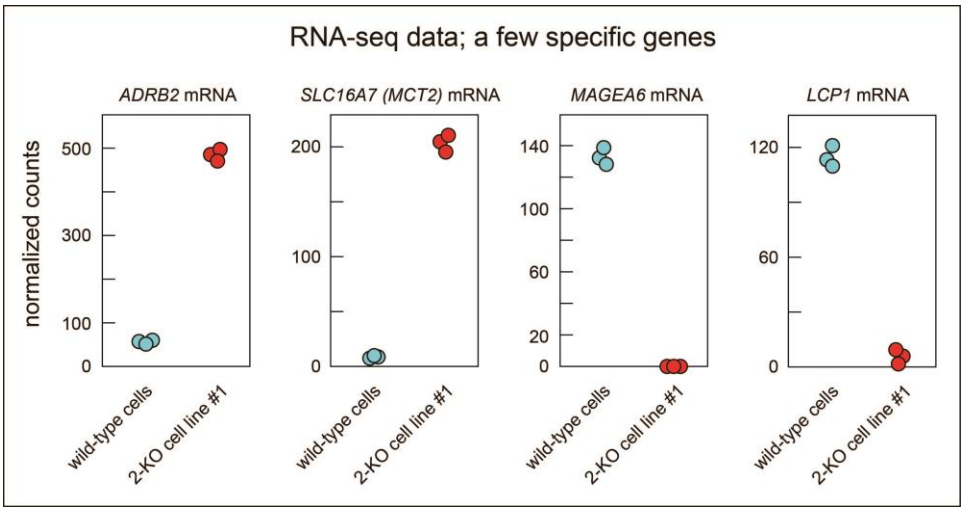

Fig. S2. Relative levels of *hsADRB2*, *hsSLC16A7 (hsMCT2)*, *hsMAGEA6*, and *hsLCP1* human mRNAs in 2-KO [*hsUBR1*$^{-/-}$ *hsUBR2*$^{-/-}$] HEK293T cells (2-KO cell line #1) (red circles) and in wild-type cells (blue circles), as measured by genome-wide RNA-seq, with three parallel and independent measurements, as indicated. See also the main text, Fig. 2D, and *SI Appendix*, Figs. S4 and S5*A*.

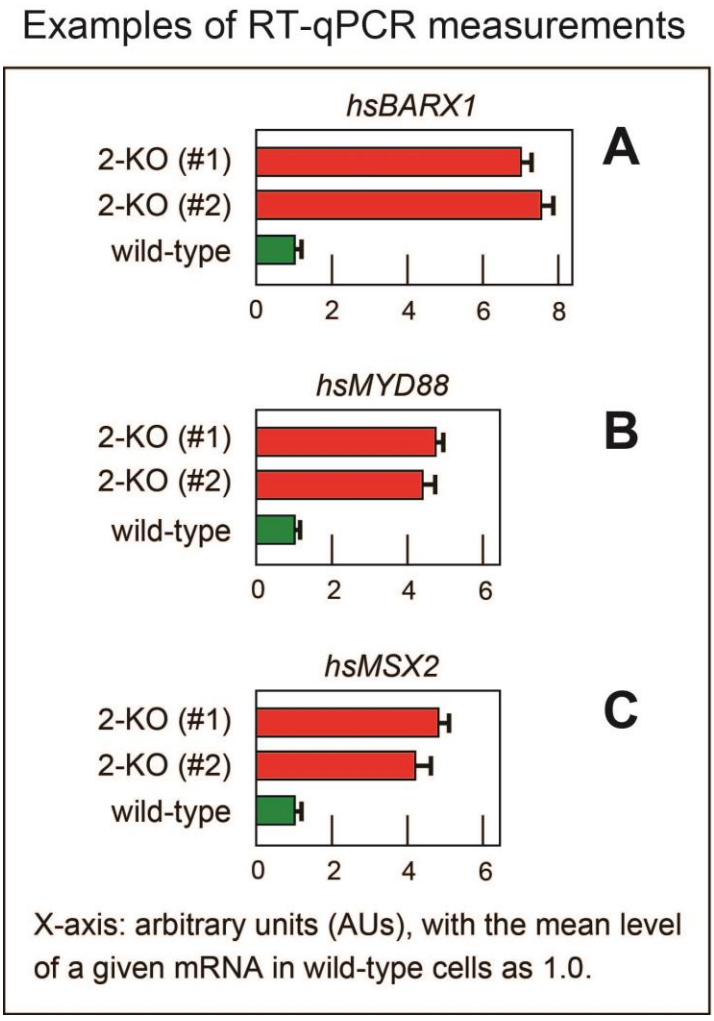

Fig. S3. Relative levels of specific human mRNAs (*hsBARX1*, *hsMYD88*, *hsMSX2*) in 2-KO [*hsUBR1*$^{-/-}$ *hsUBR2*$^{-/-}$] HEK293T cells (2-KO cell lines #1 and #2) vs. wild-type HEK293T cells, as measured by RT-qPCR. See also the main text, *SI Appendix*, Fig. S4, and Materials and Methods.

mRNAs upregulated by 2-fold or more in [*UBR1*$^{-/-}$ *UBR2*$^{-/-}$] HEK293T cells

Gene	Fold-change, in 2-KO cells	Protein; functions
SLC16A7	22.0-fold; 34.8-fold	*MCT2*; monocarboxylate (incl. lactate) transporter
ADRB2	5.9; 17.0	β-adrenergic receptor-2, recognizing catecholamines
LGALS3BP	6.2; 5.0	cell adhesion, antiviral activity
PWWP3B	5.6	unknown functions
ARMCX2	5.2	a putative mitochodrial protein
BARX1	4.9; 7.3	TF; muscle, stomach, teeth, craniofacial development
RASL10B	3.3	a RAS-like protein; likely regulator of blood pressure
NAP1L3	3.2	nucleosome assembly protein-1-like 3
CLU	3.1	a Ub-binding chaperone
MYD88	3.1; 4.6	signaling functions in the immune system
HCN2	2.9	gated K/Na-channel-2
NPTX1	2.8; 2.1	neuronal pentraxin-1; functions at excitatory synapses
RUNX3	2.7	TF; functions in neurogenesis, in T cells
SOGA3	2.7	unknown functions
CELSR3	2.6; 1.6	cadherin family member-11
DTX3	2.6	E3 Ub ligase; possible regulator of Notch
INA	2.6; 3.3	class-4 neuronal intermediate filament
PNMA3	2.6	paraneoplastic antigen-3
ACSS1	2.5	acetyl-CoA synthtetase 2-like, mitochondrial
GABRB3	2.5	GABA receptor subunit beta-3
DUSP1	2.4	dual-specificity phosphatase-1
HEXD	2.4	hexosaminidase D
TRIM25	2.4; 4.5	E3 ubiquitin/ISG15 ligase
BASP1	2.3	neuronal acidic protein, largely unknown functions
INSM1	2.3	TF; neurogenesis; cell differentiation
NPTX2	2.3	neuronal pentraxin-2
KCNQ2	2.3	voltage-gated K-channel, subfamily Q, member 2
FBF1	2.2	keratin-binding protein regulating cell polarization
GAA	2.2; 2.0	lysosomal alpha-glucosidase
JADE2	2.2	E3 Ub ligase, ubiquitylates KDM1A histone demethylase
LOC101928358	2.2	uncharacterized protein
MBNL3	2.2; 3.3	regulates alternative splicing of pre-MRNA
FOXF1	2.1	TF; transcriptional activator of lung-specific genes
H1-2	2.1	H1.2 linker histone
BAHCC1	2.1	chromatin-bound protein containing coiled-coil domain
MSX2	2.1; 4.5	TF; homeodomain; regulates bone development
SCD5	2.1	stearoyl-CoA-desaturase
RNF213	2.0	E3 Ub ligase regulating angiogenesis
ARNT2	2.0	TF; postnatal brain growth; visual and renal functions

Fig. S4. Human mRNAs that were upregulated by 2-fold or more (from 22-fold to 2-fold) in 2-KO [*hsUBR1*$^{-/-}$ *hsUBR2*$^{-/-}$] HEK293T cells (2-KO cell line #1) vs. wild-type HEK293T cells, as measured by RNA-seq, and also, for indicated mRNAs, by ^{32}P-Northern hybridization or by RT-qPCR. Values of fold-changes (second column) that were determined by RNA-seq, by ^{32}P-Northern, and by RT-qPCR are denoted, respectively, in black, red and green. In the third column, transcription factors (TF) and components of the ubiquitin-proteasome system are denoted, respectively, in red and blue. Functions of the cited proteins were compiled using entries in Uniprot (https://www.uniprot.org/) and/or GeneCards (https://www.genecards.org/). See also Fig. 2, the main text, and *SI Appendix*, Materials and Methods.

(A) mRNAs decreased (from <0.01 to 0.38) in [*UBR1*$^{-/-}$ *UBR2*$^{-/-}$] cells

Gene	Fold-change, in 2-KO cells	Protein; functions
MAGEA6	<0.01-fold;<0.01-fold	regulator of Ub ligases
MAP7D2	<0.01-fold	putative microtubule-binding protein
LCP1	0.02	actin-binding protein; apparently activates T cells
SPINT2	0.03	Kunitz type-2 serine peptidase inhibitor
AFF2	0.04	AF4/FMR2 family member-2; RNA-binding protein
SLC2A3	0.06; 0.36	facilitated glucose transporter, member 3
DDR2	0.13	discoidin domain-containing receptor-2; a Tyr kinase
TENM1	0.13	regulates, in particular, actin cytoskeletal network
PCDH9	0.23; 0.40	protocadherin-9
SERPINF1	0.23	a serpin and regulator of neuronal differentiation
B4GALT6	0.26; 0.10	synthesis of membrane-bound glycosphingolipids
RNF125	0.29; 0.43	E3 Ub ligase; ubiquitylates a number of substrates
TLE4	0.29; 0.28	TF; a corepressor that binds to a number of TFs
CYFIP2	0.31	cytoplasmic FMR1-interacting protein-2
GALNT1	0.31	N-acetylgalactosaminyltransferase-1
RUNX1T1	0.31	TF; a corepressor that binds to a number of TFs
TPGS2	0.31	subunit-2 of tubulin polyglutamylase complex
RPL22L1	0.32	ribosomal protein L22-like 1, a ribosomal component
SLC7A11	0.32	a cystine/glutamate transporter
DACH1	0.33	TF; mediates, in particular, organogenesis
ELP2	0.33	a component of RNA polymerase II elongator complex
ISL1	0.33	TF; mediates, in particular, neuronal cell differentiation
*UBR1**	0.33*	E3 Ub ligase; its gene is partly deleted in 2-KO cells*
TRAPPC8	0.34	functions in trafficking from the ER to Golgi
DSG2	0.35	component of intercellular desmosome junctions
DSC2	0.35	another component of desmosome junctions
RNF138	0.35; 0.23	E3 Ub ligase, functions in DNA damage responses
CALCB	0.36	calcitonin-related protein; induces vasodilation
DTNA	0.36	dystrobrevin-alpha
SLC6A9	0.36	importer of glycine, terminating its action at synapses
ZNF24	0.36; 0.63	TF; functions include myelination of oligodendrocytes
ZNF521	0.36	TF; functions include regulation of hematopoiesis
*UBR2**	0.37*	E3 Ub ligase; its gene is partly deleted in 2-KO cells*
ZSCAN30	0.37	a zinc finger-containing putative TF
C18orf21	0.38	uncharacterized protein
DSC3	0.38	component of intercellular desmosome junctions
PLAT	0.38	cleaves plasminogen, converting it to plasmin
MYO1C	0.38	an “unconventional” myosin

Fig. S5*A*. Human mRNAs whose relative levels were decreased (from < 0.01 to 0.38) in 2-KO [*hsUBR1*$^{-/-}$ *hsUBR2*$^{-/-}$] HEK293T cells (2-KO cell line #1) vs. wild-type cells, as measured by RNA-seq, and also, for indicated mRNAs, by ^{32}P-Northern hybridization or by RT-qPCR. This is the first part (*A*) of the multipart (*A*-*C*) Fig. S5. Asterisks by *UBR1** and *UBR2** (first column) refer to protein-ablating (Fig. 2A and *SI Appendix*, Fig. S10) (but not eliminating all *hsUBR1*/*hsUBR2* RNA) partial deletions of both *hsUBR1* and *hsUBR2* in 2-KO HEK293T cells (1). Values of fold-changes (second column) that were determined by either RNA-seq, ^{32}P-Northern, or RT-qPCR are, respectively, in black, red and green. In the third column, transcription factors (TF) and components of the ubiquitin-proteasome system are in red and blue, respectively. Functions of the cited proteins were compiled using entries in Uniprot (https://www.uniprot.org/) and/or GeneCards (https://www.genecards.org/). See also Fig. 2, the main text, and *SI Appendix*, Materials and Methods.

(B) mRNAs decreased (from 0.39 to 0.48) in [*UBR1*$^{-/-}$ *UBR2*$^{-/-}$] cells

Gene	Fold-change, in 2-KO cells	Protein; functions
F2RL1	0.39-fold	protease-activated receptor-2; functions in immunity
MAPRE2	0.39	microtubule-associated protein RP/EB member-2
SLC8A1	0.39	sodium/calcium exchanger-1
EN2	0.40; 0.49	TF; homeobox protein engrailed-2
ZNF397	0.40	TF; functions unknown
GAREM1	0.41	regulates activation of the MAPK/ERK pathway
GPC3	0.41	glypican-3; cell-surface proteoglycan
NHSL1	0.41	NHS-like protein-1; unknown functions
RPRD1A	0.41	binds to phosphorylated CTD domain of RNA Pol II
INO80C	0.41	subunit of Ithe NO80 chromatin remodeling complex
SLC39A6	0.41	zinc transporter (ZIP6)
VCAN	0.41	versican protein; a role in cell-matrix connections
ZBED6CL	0.41	encoded by a DNA transposon; unclear functions
PANX2	0.42	pannexin-2
SLITRK5	0.42	suppresses neurite outgrowth
TTC26	0.42	required for transport of proteins in the motile cilium
YBX1	0.42	TF; mutifunctional DNA/RNA-binding regulator
CABLES1	0.43	CDK kinase-binding regulatory protein
GPC6	0.43	a cell-surface proteoglycan
CDH2	0.44; 0.52	a calcium-dependent cell adhesion protein
INSIG1	0.44	mediates feedback control of cholesterol synthesis
OSBPL1A	0.44	oxysterol-binding protein-related protein-1
RUSC2	0.44	RUN and SH3 domains-containing protein-2
SLC37A3	0.44	sugar-phosphate exchanger-3
SLAIN1	0.44	microtubule plus-end tracking protein
TBC1D4	0.44	a GTPase-activating protein for RAB-family proteins
THRB	0.44	thyroid hormone receptor-beta
TMEM178B	0.44	transmembrane protein 178B; unknown functions
LMBR1	0.45	transmembrane protein; functions unclear
PRDM6	0.45	putative histone methyltransferase
TAOK3	0.45	Ser/Thr-kinase and regulator of p38/MAPK14 cascade
TSHZ3	0.45	TF; functions as a gene repressor during development
MIER2	0.46	mesoderm induction early response protein-2
PAPSS2	0.46	3'-phosphoadenosine 5'-phosphosulfate synthase-2
FHOD3	0.47	actin-organizing protein
FLRT3	0.47	functions in cell-cell adhesion and axon guidance
BAX	0.48	regulator of apoptosis
DIS3	0.48	exoribonuclease

Fig. S5*B*. *Continuation of Fig. S5A*. Human mRNAs whose relative levels were decreased (from 0.39 to 0.48) in 2-KO [*hsUBR1*$^{-/-}$ *hsUBR2*$^{-/-}$] HEK293T cells (2-KO cell line #1) vs. wild-type HEK293T cells, as measured by RNA-seq, and also, for indicated mRNAs, by RT-qPCR. Values of fold-changes (second column) that were determined by RNA-seq and by RT-qPCR are in black and green, respectively. In the third column, transcription factors (TF) and components of the ubiquitin-proteasome system are, respectively, in red and blue. Functions of the cited proteins were compiled using entries in Uniprot (https://www.uniprot.org/) and/or GeneCards (https://www.genecards.org/). See also Fig. 2, the main text, and *SI Appendix*, Materials and Methods.

(C) mRNAs decreased (from 0.48 to 0.50) in [*UBR1*$^{-/-}$ *UBR2*$^{-/-}$] cells

Gene	Fold-change, in 2-KO cells	Protein; functions
FKBP10	0.48-fold	peptidyl-prolyl cis-trans isomerase
GPR180	0.48	a G protein-coupled receptor
LRATD2	0.48	a transmembrane protein; functions unknown
OBSCN	0.48	obscurin, a structural protein in striated muscle
ABCB8	0.49	ATP-binding subunit of a mitochondrial K-channel
ATP6V0E2	0.49	a subunit of a vacuolar-type acidifying ATPase
KLF12	0.49	TF; a Krueppel-like transcriptional repressor
MAF	0.49; 0.65	TF; functions as either activator or repressor
MCC	0.49	a tumor suppressor and regulator of the Wnt pathway
NR2F1	0.49	TF; functions as either activator or repressor
TMED7	0.49	a transmembrane protein; roles in vesicular transport
ZYX	0.49	zyxin; an adhesion plaque protein; binds alpha-actinin
AP1S2	0.50	a subunit of clathrin-associated adaptor complex
CITED1	0.50	TF; coactivator of the p300/CBP complex
GPX8	0.50	a probable glutathione peroxidase
LHFPL2	0.50	functions in female and male fertility
RPS23	0.50	ribosomal protein of the 40S ribosomal subunit

Fig. S5C. *Continuation of Fig. S5A, B.* Human mRNAs whose relative levels were decreased (from 0.48 to 0.50) in 2-KO [*hsUBR1*$^{-/-}$ *hsUBR2*$^{-/-}$] HEK293T cells (2-KO cell line #1) vs. wild-type HEK293T cells, as measured by RNA-seq, and also, for one mRNA, by RT-qPCR. Values of fold-changes (second column) that were determined by RNA-seq and by RT-qPCR are in black and green, respectively. In the third column, transcription factors (TF) and components of the ubiquitin-proteasome system are, respectively, in red and blue. Functions of the cited proteins were compiled using entries in Uniprot (https://www.uniprot.org/) and/or GeneCards (https://www.genecards.org/). See also Fig. 2, the main text, and *SI Appendix*, Materials and Methods.

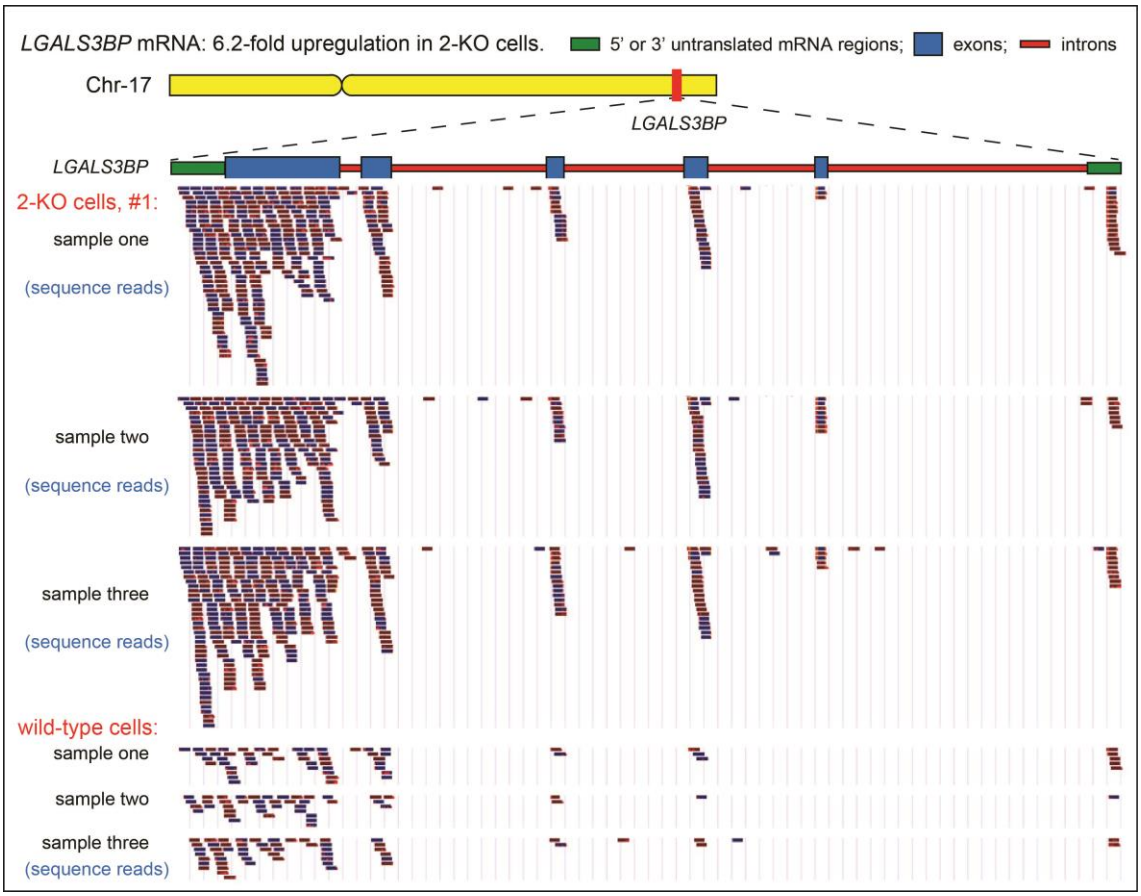

Fig. S6. Sets of sequence "reads", by genome-wide, Illumina instrument-based RNA-seq measurements, for the example of human *LGALS3BP* mRNA in 2-KO [*hsUBR1*$^{-/-}$ *hsUBR2*$^{-/-}$] HEK293T cells (2-KO cell line #1) (upper three sets) vs. wild-type HEK293T cells (lower three sets), as indicated on the diagram. *LGALS3BP* encodes a protein that functions in cell adhesion and immune responses. *LGALS3BP* mRNA was increased by ~6-fold in 2-KO cells, relative to wild-type cells (Fig. 2D and *SI Appendix*, Fig. S4). *LGALS3BP* is located on the long arm of human chromosome 17. The intron-exon configuration of the *LGALS3BP* gene is also shown, with introns (to scale) in red. As would be expected, given the RNA-seq technology and its use for mRNA quantification (2-4), virtually all sequence reads for *LGALS3BP* are confined to its mRNA's protein-coding exons (in blue) or to mRNA's 5'- and 3'-noncoding regions (in green) in both 2-KO and wild-type cells. Note the relative scarcity of sequence reads for wild-type cells (the lower three sets), in which the level of *LGALS3BP* mRNA is 6.2-fold lower than in 2-KO cells. See also the main text, Fig. 2D, and *SI Appendix*, Fig. S4.

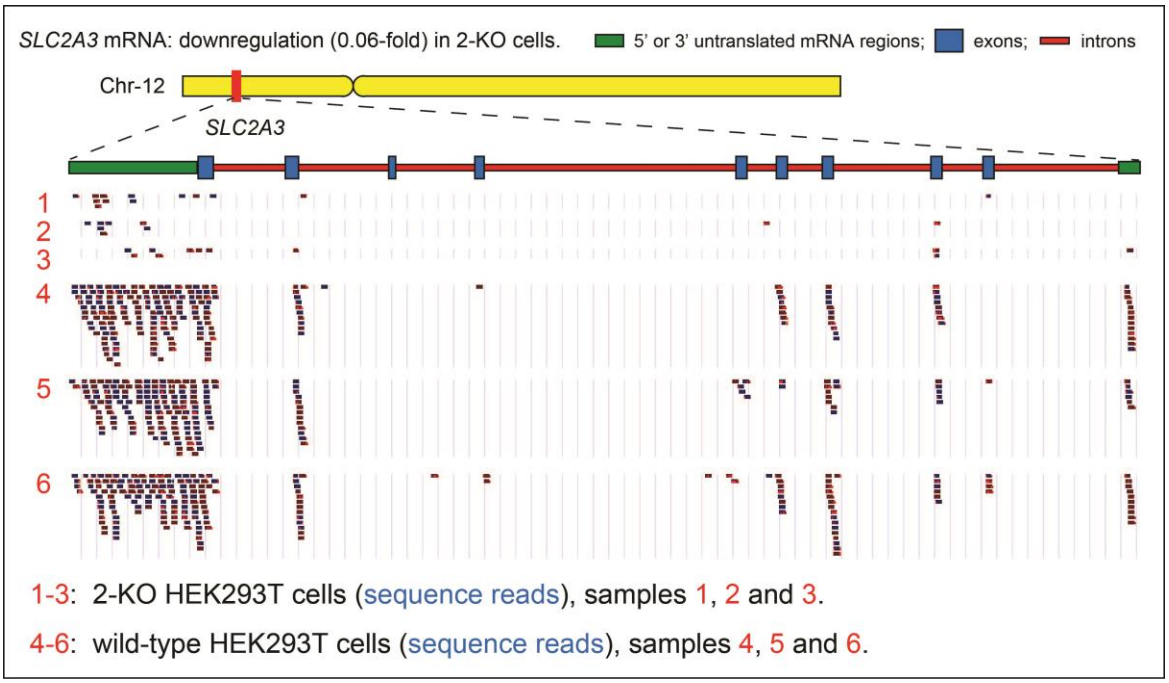

Fig. S7. Second example (see Fig. S6 for the first one) of sequence "reads", by genome-wide, Illumina instrument-based RNA-seq measurements of human *SLC2A3* mRNA in 2-KO [*hsUBR1*$^{-/-}$ *hsUBR2*$^{-/-}$] HEK293T cells (2-KO cell line #1) (upper three sets, 1-3) vs. wild-type cells (lower three sets, 1-3), as indicated on the diagram. *SLC2A3* encodes a glucose transporter (Fig. 2D and *SI Appendix*, Fig. S5A). In contrast to *LGALS3BP* mRNA (*SI Appendix*, Fig. S6), which was increased by ~6-fold in 2-KO cells, relative to wild-type cells, *SLC2A3* mRNA was decreased by ~16-fold in 2-KO cells (Fig. 2D and *SI Appendix*, Fig. S5A). The *SLC2A3* gene is located on the short arm of human chromosome 12. The intron-exon configuration of *SLC2A3* is also shown, with introns (to scale) in red. As would be expected, given the RNA-seq technique and its use for mRNA quantification, virtually all sequence reads for *SLC2A3* are confined to its mRNA's protein-coding exons (in blue) or to mRNA's 5'- and 3'-noncoding regions (in green) in both 2-KO and wild-type cells. Note the scarcity of sequence reads for 2-KO cells (the upper three sets), in which the level of *SLC2A3* mRNA is ~16-fold lower than in wild-type cells, a pattern "opposite" to the one for the *LGALS3BP* gene, in *SI Appendix*, Fig. S6. See also the main text, Fig. 2D, and *SI Appendix*, Fig. S5A.

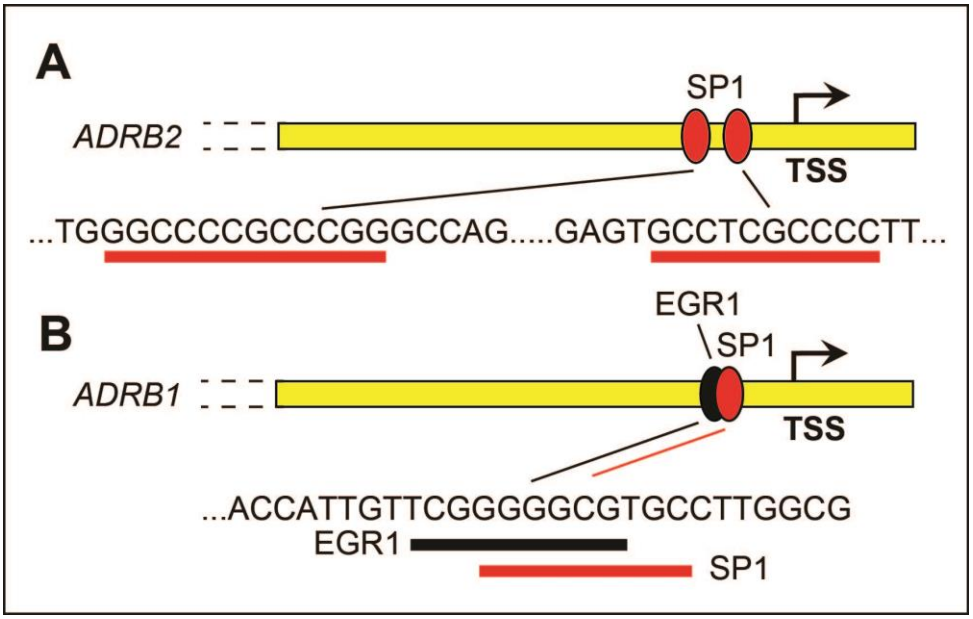

Fig. S8. Promoters of the human *hsADRB1* and *hsADRB2* genes. Only TSS (main transcription start site)-proximal regions are shown. (*A*) *hsADRB2* contains two sites for the *hs*SP1 activator TF (red ovals) and also, potentially importantly, lacks the binding site for the *hs*EGR1 repressor TF (black oval in *hsADRB1*) (5-9). (*B*) hs*ADRB1* contains one *hs*SP1 site and the partially overlapping *hs*EGR1 site, so that the binding of *hs*SP1 activator and *hs*EGR1 repressor to *hsADRB1* is expected to be mutually exclusive. This working model, which remains to be verified experimentally, may account, at least in part, for the observed 17-fold increase of *hsADRB2* mRNA but not of *hsADRB1* mRNA in 2-KO HEK293T cells (see the main text, Fig. 2, and *SI Appendix*, Fig. S4). DNA sequences of (overlapping) sites that are recognized by *hs*SP1 and *hs*EGR1 are underlined in red and black, respectively. Not shown are several non-*hs*SP1, non-*hs*EGR1 TF-binding sites that do not differ significantly between *hsADRB1* and *hsADRB2*.

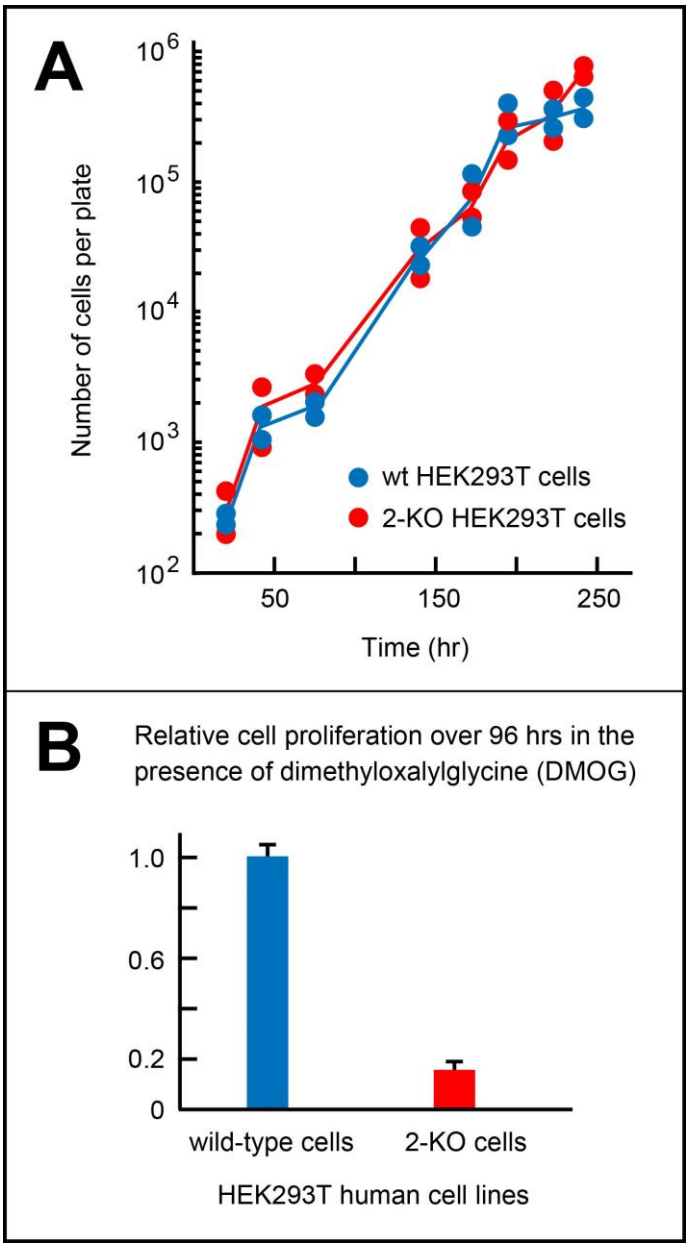

Fig. S9. Human 2-KO [*hsUBR1*$^{-/-}$ *hsUBR2*$^{-/-}$] HEK293T cells, which overexpress both *hsMCT2* (*hsSLC16A7*) mRNA and *hsMCT2* protein (a monocarboxylate transporter) (Fig. 2 and *SI Appendix*, Figs. S4 and S12*A*), are hypersensitive to dimethyloxalylglycine (DMOG). (*A*) Similar growth rates of wild-type and 2-KO HEK293T cells under normal conditions. Duplicate samples of wild-type and 2-KO cells were seeded onto plates, and their numbers were determined as a function of time, as described in *SI Appendix*, Materials and Methods. (*B*) Hypersensitivity of 2-KO HEK293T cells to dimethyloxalylglycine (DMOG), whose derivative methyloxalylglycine (MOG) is transferred into cells largely by the *hs*MCT2 (*hs*SLC16A7) transporter (Fig. 2 and *SI Appendix*, Figs. S4 and S12*A*). See the main text for biochemical strategy and rationale of this assay.

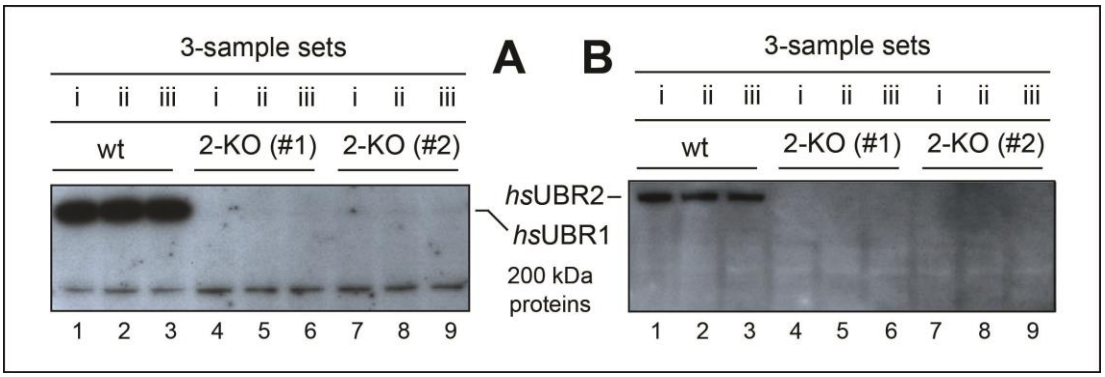

Fig. S10. Immunoblot (IB) analyses, using anti-UBR1 and anti-UBR2 antibodies, of extracts from 2-KO [*hsUBR1*$^{-/-}$ *hsUBR2*$^{-/-}$] HEK293T cells and their wild-type counterparts prior to proteome-wide mass spectrometric (TMT-SPS-MS3) comparisons of these extracts. (*A*) Lanes 1-3, IB, with antibody to *hs*UBR1, of three extracts from three independently grown samples (i-iii) of wild-type HEK293T cells. Lanes 4-6, same as lanes 1-3, but with extracts from three samples of 2-KO HEK293T cells (2-KO cell line #1). Lanes 7-9, same as lanes 4-6 but with 2-KO cell line #2. (*B*) Lanes 1-9, same as lanes 1-9 in *A*, but IB with antibody to *hs*UBR2. See *SI Appendix*, Materials and Methods for additional details.

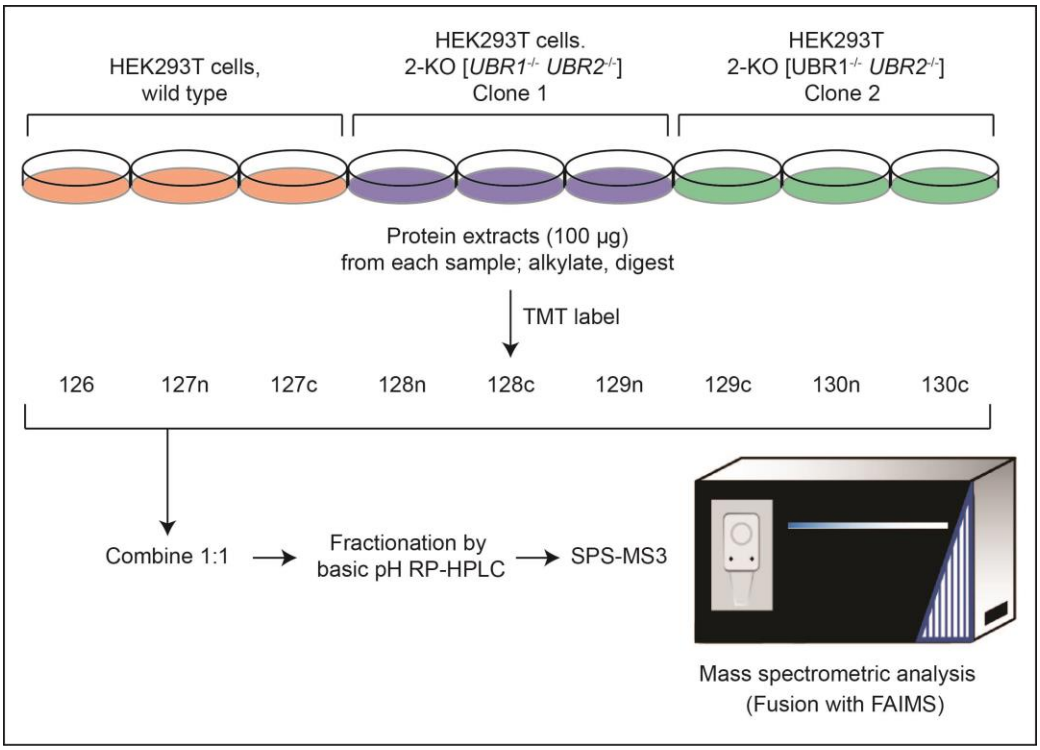

Fig. S11. Summary of MS analyses using TMT-SPS-MS3 (10). See *SI Appendix*, Materials and Methods for additional details.

(A) MS analyses: proteins upregulated by 2-fold or more in [*UBR1*$^{-/-}$ *UBR2*$^{-/-}$] HEK293T cells

Protein	Fold-change, in 2-KO cell line #1	Fold-change, in 2-KO cell line #2	RNA-seq, in #1, fold-change	Protein; functions
MCT2	6.0-fold	2.7-fold	22-fold	SLC16A7; monocarboxylate transporter
LRRC58	4.2	3.3	NA*	a protein containing leucine-rich repeats
MAMLD1	3.0	1.6	2.3	TF; activates the promoter of *HES3* gene
AP3B2	2.9	2.1	NA*	subunit of non-clathrin AP3 adaptor complex
STMN3	2.9	3.5	0.65	stathmin-3; microtubule-destabilizing activity
CKMT1A	2.7	2.7	NA*	mitochondrial creatine kinase, U-type
DPYSL4	2.7	1.3	NA*	a role in signaling by class 3 semaphorins
CENPV	2.6	1.7	NA*	a component of chromosomal centromeres
SDCCAG8	2.6	2.2	NA*	a role in ciliogenesis and Hedgehog pathway
NQO1	2.5	1.4	NA*	a quinone reductase; detoxification pathways
SARM1	2.5	2.0	NA*	NAD(+) hydrolase; a role in axonal degeneration
DCLK2	2.5	1.2	NA*	Ser/Thr-kinase; reduced affinity for camodulin(Ca)
CRYL1	2.4	2.0	NA*	a homolog of lambda-crystallin
DLGAP5	2.4	1.3	NA*	a spindle-localized potential cell cycle regulator
INA	2.4	1.2	2.6	alpha-internexin; subunit of some neurofilaments
PPDPF	2.4	1.2	NA*	a regulator of exocrine pancreas development
SLC25A29	2.3	1.5	1.6	mitochondrial transporter of basic amino acids
VIPR1	2.3	1.2	1.6	a receptor for vasoactive intestinal peptide (VIP)
ACAD11	2.3	1.4	NA*	an acyl-CoA dehydrogenase
DNAJB5	2.4	1.2	NA*	a DNAJ-like chaperone
GNG4	2.3	2.8	1.3	a gamma-subunit of specific G proteins
TBC1D5	2.6	1.2	1.5	a putative GTPase-activating protein (GAP)
PXDN	2.2	1.6	1.9	a sequelog of peroxidasin; unknown functions
TRPM5	2.2	1.6	NA*	Ca(2+)-activated, monovalent cation channel
NECAB3	2.2	2.3	NA*	EF-hand calcium-binding protein-3
RBKS	2.2	1.9	NA*	ribokinase; phosphorylation of ribose at oxygen-5
NFIC	2.2	1.6	1.8	TF; recognizes 5'-TTGGCNNNNNGCCAA-3'
BPHL	2.2	1.8	1.8	valacyclovir hydrolase; a likely detoxifying enzyme
CBX5	2.1	1.6	1.5	histone reader, recognizing methylated histone H3
MYEF2	2.1	1.4	1.5	TF; represses myelin basic protein (MBP) gene
ERAP2	2.1	1.3	NA*	aminopeptidase in the ER, and also in the cytosol
ENPP5	2.1	1.4	NA*	ectonucleotide phosphodiesterase

Fig. S12*A*. MS analyses, using TMT-SPS-MS3 (10). Human proteins whose relative levels were increased (from 6-fold to 2.1-fold) in 2-KO [*hsUBR1*$^{-/-}$ *hsUBR2*$^{-/-}$] HEK293T cells (2-KO cell line #1 and 2-KO cell line #2) vs. wild-type HEK292T cells, are cited in the second and third columns, respectively. The entries are cited in the order of fold-values determined for 2-KO cell line #1 vs. wild-type HEK293T cells. Fold-values for the corresponding mRNAs, determined by RNA-seq (with RNA from 2-KO cell line #1 vs. RNA from wild-type cells) are cited in the fourth column. NA* ("not applicable") refers to the absence of detectable mRNA levels in both 2-KO and wild-type cell lines. In the fifth column, transcription factors (TFs) are denoted in red. Functions of the cited proteins were compiled using entries in Uniprot (https://www.uniprot.org/) and/or GeneCards (https://www.genecards.org/). See also Fig. 2, the main text, and *SI Appendix*, Materials and Methods.

Note qualitative agreement between the finding of upregulated (by 22-fold) *hsMCT2* mRNA (encoding a monocarboxylate transporter; Fig. 2 and *SI Appendix*, Fig. S4) and the also upregulated *hs*MCT2 protein (by 6-fold and 2.7-fold, in 2-KO cell lines), as determined by MS. See the main text for additional details.

(B) MS analyses: proteins upregulated by 2-fold or more in [*UBR1*$^{-/-}$ *UBR2*$^{-/-}$] HEK293T cells

Protein	Fold-change, in 2-KO cell line #1	Fold-change, in 2-KO cell line #2	RNA-seq, in #1, fold-change	Protein; functions
SERPINI1	2.1-fold	2.5-fold	3.6	neuroserpin, a serine protease inhibitor
PYGL	2.1	1.4	1.3	glycogen phosphorylase
CAV1	2.0	1.8	1.7	a scaffolding protein within caveolar membranes
AGMAT	2.0	1.1	2.1	agmatinase; from agmatine to putrescine
A2M	2.0	2.8	NA*	alpha-2-macroglobulin, a protease inhibitor
BICC1	2.0	1.8	1.5	RNA-binding protein; a regulator of Wnt signaling
HSPA1L	2.0	1.8	NA*	one of Hsp70 chaperones
CNRIP1	2.0	1.4	1.6	a cannabinoid receptor-interacting protein
CAP2	2.0	1.3	NA*	a protein that interacts with adenylyl cyclase
SMPD1	2.0	0.8	NA*	enzyme that converts sphingomyelin to ceramide
PLA2G6	1.9	2.5	NA*	calcium-independent phospholipase A2

Fig. S12*B*. *Continuation of Fig. S12A.* MS analyses, using TMT-SPS-MS3 (10). Human proteins whose relative levels were increased (from 2.1-fold to 2.0-fold) in 2-KO [*hsUBR1*$^{-/-}$ *hsUBR2*$^{-/-}$] HEK293T cells (2-KO cell line #1 and 2-KO cell line #2) vs. wild-type HEK292T cells are cited in the second and third columns, respectively. The entries are cited in the order of fold-values determined for 2-KO cell line #1 vs. wild-type HEK293T cells. Fold-values for the corresponding mRNAs, determined by RNA-seq (with RNA from 2-KO cell line #1 vs. RNA from wild-type cells) are cited in the fourth column. NA* ("not applicable") refers to the absence of detectable mRNA levels in both 2-KO and wild-type cell lines. Functions of the cited proteins were compiled using entries in Uniprot (https://www.uniprot.org/) and/or GeneCards (https://www.genecards.org/). See also Fig. 2, the main text, and *SI Appendix*, Materials and Methods.

Although, the last entry, *hs*PLA2G6 (calcium-independent phospholipase A2), was upregulated, according to MS data, by less than 2-fold in 2-KO cell line #1, it was upregulated by 2.5-fold in 2-KO cell line #2. In addition, *hs*PLA2G6 is a protein whose natural fragments, produced by caspases under apoptotic and other conditions, are likely to be substrates of the Arg/N-degron pathway (11, 12).

(A) MS analyses: proteins decreased (from <0.01 to 0.36) in [*UBR1*$^{-/-}$ *UBR2*$^{-/-}$] cells

Protein	Fold-change, in 2-KO cell line #1	Fold-change, in 2-KO cell line #2	RNA-seq, in #1, fold-change	Protein; functions
MAGEA6/10	<0.01-fold	<0.01-fold	NA*	MAGEA6 & 10 are highly sequelogous; see legend
FAM84B	<0.02-fold	0.04-fold	0.48	(LRATD2); often overexpressed in cancers
NF-M	0.06	0.06	1.7	(NFEM); subunit of neurofilaments
NF-L	0.06	0.05	1.2	(NFEL); another subunit of neurofilaments
RENBP	0.07	0.06	NA*	N-acylglucosamine 2-epimerase
MYOM2	0.10	0.23	NA*	myomesin-2, a component of myofibrillar M-band
DPYSL3	0.14	0.10	NA*	functions in cell migration and axon guidance
KCTD12	0.16	0.15	0.56	auxiliary subunit of GABA receptors
MOCOS	0.16	0.13	0.35	sulfurates the molybdenum cofactor
MAP7D2	0.16	0.19	<0.01	putative microtubule-binding protein
CDYL2	0.16	0.09	NA*	ribokinase; phosphorylation of ribose at oxygen-5
POTEI	0.18	0.17	NA*	an ankyrin domain family member
PCDH9	0.19	0.19	0.23	protocadherin-9, a cell adhesion protein
DACH1	0.20	0.35	0.26	TF; mediates, in particular, organogenesis
ICAM1	0.22	0.20	NA*	a ligand for for leukocyte adhesion protein LFA1
SH2D4A	0.23	0.27	0.33	inhibits estrogen-induced cell proliferation
APOBEC3B	0.27	0.04	0.51	dU-editing enzyme (cytidine deaminase)
SLITRK5	0.28	0.28	0.42	suppresses neurite outgrowth
KLF5	0.29	0.40	0.55	TF; Kruppel-like; binds to GC-box promoters
GAREM	0.29	0.30	0.41	GRB2-associated; regulator of MAPK protein 1
GALNT1	0.30	0.28	0.31	mediates O-linked oligosaccharide biosynthesis
LCP1	0.31	0.19	0.02	activation of T cells
DTNA	0.32	0.34	0.36	dystrobrevin-alpha; a role in synapses
MCC	0.33	0.52	0.49	putative colorectal tumor suppressor, at 5q21
RBM47	0.33	0.44	0.50	RNA-binding protein; unknown functions
COL14A1	0.34	0.26	0.41	collagen alpha-1 (XIV) chain
PRDM6	0.34	0.68	0.45	TF; repressor of smooth muscle gene expression
BAX	0.36	0.58	0.48	regulator of mitochondria-mediated apoptosis

Fig. S13*A*. MS analyses, using TMT-SPS-MS3 (10). Human proteins whose levels were decreased (from <0.01-fold to 0.36-fold) in 2-KO HEK293T cells (2-KO cell line #1 and 2-KO cell line #2) vs. wild-type HEK292T cells are cited in the second and third columns, respectively. The entries are cited in the order of fold-values determined for 2-KO cell line #1 vs. wild-type HEK293T cells. Fold-values for corresponding mRNAs, determined by RNA-seq (with RNA from 2-KO cell line #1 vs. RNA from wild-type cells) are cited in the fourth column. NA* ("not applicable") refers to the absence of detectable mRNA levels in both 2-KO and wild-type cell lines. In the fifth column, transcription factors (TFs) are denoted in red. Functions of the cited proteins were compiled using entries in Uniprot (https://www.uniprot.org/) and/or GeneCards (https://www.genecards.org/). See also Fig. 2, the main text, and *SI Appendix*, Materials and Methods.

See the main text for discussion of the observed, by MS, of a strong downregulation (<0.01-fold) *hs*MAGEA6 and/or *hs*MAGEA10. The two proteins are 49% identical and distinguishing between them by MS is not a straightforward task. Hence, NA* ("not applicable") in the fourth column in regard to a corresponding mRNA fold-value, although *hsMAGEA6* mRNA was shown, using both RNA-seq and ^{32}P-Northerns, to be strongly (<0.01-fold) downregulated in both 2-KO cell line #1 and 2-KO cell line #2, in comparison to wild-type HEK293T cells (Fig. 2*E, D*). It is likely (but remains to be verified), that an *hs*MAGEA6/10 protein that was strongly (<0.01-fold) downregulated in 2-KO cells was, in fact, the *hs*MAGEA6 protein. We do not know, as yet, whether *hsMAGEA10* mRNA was also downregulated in 2-KO cells, similarly to *hsMAGEA6* mRNA (Fig. 2*E, D*).

(B) MS analyses: proteins decreased (from 0.36 to 0.42) in [*UBR1* $^{-/-}$ *UBR2* $^{-/-}$] cells

Protein	Fold-change, in 2-KO cell line #1	Fold-change, in 2-KO cell line #2	RNA-seq, in #1, fold-change	Protein; functions
SNX18	0.36-fold	0.59-fold	0.59	endicytosis and intracellular vesivle trafficking
PRAME	0.36	0.49	NA*	TF; inhibits signaling by retinoic acid
HLA-DMA	0.37	0.19	NA*	functions in releasing CLIP peptide from MHC II
ATP2B4	0.37	0.30	0.73	ATPase; exports calcium ions from cells
MYO1C	0.37	0.39	0.38	unconventional myosin; role in insulin pathways
FKBP10	0.37	0.24	0.48	peptidyl-prolyl cis-trans isomerase
PIP	0.37	0.36	NA*	prolactin-iducible protein; unknown functions
KLHL11	0.37	0.41	NA*	subunit of a cullin-RING-based E3 ubiquitin ligase
CA2	0.37	0.87	NA*	carbonic anhydrase-2
RASSF5	0.38	0.31	NA*	RAS-like protein; possible tumor suppressor
DSG2	0.38	0.39	0.35	component of intercellular desmosome junctions
RNF138	0.39	0.51	0.35	E3 ubiquitin ligase; role in DNA damage response
GPC6	0.39	0.30	0.43	component of cell surface proteoglycan
SULT1A3	0.39	0.23	NA*	sulfotransferase; substrates include dopamine
FBXO17	0.40	0.80	0.55	recognition component of SCF ubiquitin ligase
TPD52L1	0.40	0.41	NA*	unknown functions
TMEM97	0.40	0.40	NA*	intracellular protein that binds to numerous drugs
BCAM	0.40	0.78	NA*	receptor for laminin alpha-5
TBC1D4	0.40	0.49	NA*	may be a specific GTPase-activating protein
DSC2	0.40	0.35	0.35	component of intercellular desmosome junctions
RPRD1A	0.41	0.39	0.41	regulator of RNA polymerase II
RBPMS2	0.41	0.46	NA*	RNA-binding protein; roles in cell differentiation
QPCT	0.49	0.26	0.31	bosynthesis of pyroglutamyl peptides
SLC16A2	0.41	0.25	1.4	thyroid hormone transporter
MRM1	0.41	0.37	NA*	methylates mitochondrial rRNA
ARHGAP8	0.41	0.95	NA*	GTPase activator for specific Rho-type GTPases
TGM2	0.42	0.28	NA*	catalyzes cross-linking of specific proteins
KLC3	0.42	0.53	NA*	light chain of kinesin, a microtubule-bound enzyme

Fig. S13*B*. *Continuation of Fig.* S13*A*. MS analyses, using TMT-SPS-MS3 (10). Human proteins whose relative levels were decreased (from <0.36-fold to 0.42-fold) in 2-KO [*hsUBR1* $^{-/-}$ *hsUBR2* $^{-/-}$] HEK293T cells (2-KO cell line #1 and 2-KO cell line #2) vs. wild-type HEK292T cells are cited in the second and third columns, respectively. The entries are cited in the order of fold-values determined for 2-KO cell line #1 vs. wild-type HEK293T cells. Fold-values for corresponding mRNAs, determined by RNA-seq (with RNA from 2-KO cell line #1 vs. RNA from wild-type cells) are cited in the fourth column. NA* ("not applicable") refers to the absence of detectable mRNA levels in both 2-KO and wild-type cell lines. In the fifth column, transcription factors (TFs) and components of the ubiquitin-proteasome system are in red and blue, respectively. Functions of the cited proteins were compiled using entries in Uniprot (https://www.uniprot.org/) and/or GeneCards (https://www.genecards.org/). See also Fig. 2 and *SI Appendix*, Materials and Methods.

(C) MS analyses: proteins decreased (from 0.42 to 0.47) in [*UBR1*$^{-/-}$ *UBR2*$^{-/-}$] cells

Protein	Fold-change, in 2-KO cell line #1	Fold-change, in 2-KO cell line #2	RNA-seq, in #1, fold-change	Protein; functions
HOXA13	0.42-fold	0.64-fold	0.50	TF; contributes to specifying anterior-posterior axis
BBS10	0.42	0.44	NA*	probable molecular chaperone
MAPRE2	0.42	0.40	0.39	microtubule-associated protein, of RP/EB family
CRABP2	0.42	0.46	1.41	transports retinoic acid to the nucleus
GSTK1	0.43	0.51	0.61	glutathione S-transferase kappa-1
CPPED1	0.43	0.24	NA*	Ser/Thr-protein phosphatase
DUSP9	0.43	0.45	NA*	dual-specificity protein phosphatase-9
HPCAL4	0.44	0.40	NA*	hippocalcin-like protein-4; unknown functions
RSAD1	0.44	0.56	NA*	unclear functions; may be a heme chaperone
NDRG1	0.44	0.69	0.83	a tumor suppressor; specific functions unknown
SEPHS2	0.44	0.34	0.88	enzyme; selenophosphate from selenide and ATP
NRP2	0.44	0.37	NA*	receptor for semaphorins and other proteins
MRC2	0.45	0.25	0.52	C-type mannose receptor
DIS3	0.45	0.45	0.48	component of RNA exosome; possible nuclease
ADRBK2	0.45	0.74	NA*	G protein-coupled receptor kinase
NAGA	0.45	0.52	0.71	alpha-N-acetylgalactosaminidase
MYCBP2	0.46	0.44	0.66	E3 ubiquitin ligase; ubiquitylates Ser/Thr
MIPEP	0.46	0.56	NA*	mitochondrial “intermediate” peptidase
CEP72	0.46	0.71	NA*	a component of centrosome
LEPREL2	0.46	0.72	NA*	component of a prolyl 3-hydroxylase
ALDH1A2	0.46	0.61	0.65	enzyme; converts retinaldehyde to retinoic acid
TTC39A	0.46	0.35	NA*	unknown functons
ZNF24	0.46	0.50	0.36	TF; required for myelination of oligodendrocytes
PNKP	0.46	1.0	NA*	bifunctional polynucleotide phosphatase/kinase
RHOBTB3	0.46	0.81	0.53	ATPase required for endosome to Golgi transport
SEC14L2	0.47	0.76	NA*	carrier; binds to specific hydrophobic compounds
HMOX1	0.47	0.40	NA*	heme oxygenase-1
ABCB8	0.47	0.74	0.49	subunit of mitochondrial potassium channel

Fig. S13*C*. *Continuation of Fig.* S13*A-B*. MS analyses, using TMT-SPS-MS3 (10). Human proteins whose relative levels were decreased (from <0.42-fold to 0.47-fold) in 2-KO [*hsUBR1*$^{-/-}$ *hsUBR2*$^{-/-}$] HEK293T cells (2-KO cell line #1 and 2-KO cell line #2) vs. wild-type HEK292T cells are cited in the second and third columns, respectively. The entries are cited in the order of fold-values determined for 2-KO cell line #1 vs. wild-type HEK293T cells. Fold-values for corresponding mRNAs, determined by RNA-seq (with RNA from 2-KO cell line #1 vs. RNA from wild-type cells) are cited in the fourth column. NA* (“not applicable”) refers to the absence of detectable mRNA levels in both 2-KO and wild-type cell lines. In the fifth column, transcription factors (TFs) and components of the ubiquitin-proteasome system are in red and blue, respectively. Functions of the cited proteins were compiled using entries in Uniprot (https://www.uniprot.org/) and/or GeneCards (https://www.genecards.org/). See also Fig. 2 and *SI Appendix*, Materials and Methods.

(D) MS analyses: proteins decreased (from 0.47 to 0.50) in [*UBR1*$^{-/-}$ *UBR2*$^{-/-}$] cells

Protein	Fold-change, in 2-KO cell line #1	Fold-change, in 2-KO cell line #2	RNA-seq, in #1, fold-change	Protein; functions
PLTP	0.47-fold	0.66-fold	NA*	phospholipid transfer protein
QPRT	0.48	0.13	NA*	nicotinate-nucleotide pyrophosphorylase
UBR3	0.48	0.70	NA*	E3 ubiquitin ligase; a sequelog of UBR1/UBR2
INPP5K	0.48	0.49	NA*	inositol polyphosphate 5-phosphatase
TTC38	0.48	0.80	0.75	unknown functions
IRS2	0.48	0.48	NA*	a component of insulin signaling pathway
SHKBP1	0.48	0.89	NA*	a part of EGF receptor signaling pathways
NOVA2	0.48	0.62	NA*	RNA-binding protein; may regulate RNA splicing
EIF2D	0.48	0.59	0.63	translation initiation factor-2D
SDK2	0.48	0.72	NA*	adhesion protein in retinal synaptic connections
TACC2	0.48	0.44	NA*	a role in coupling the nucleus and the centrosome
CHEK2	0.48	0.78	NA*	Ser/Thr-protein kinase CHK2
LEPREL4	0.45	0.25	NA*	component of a prolyl 3-hydroxylase
UCHL3	0.49	0.37	0.51	a deubiquitylating enzyme (DUB)
RBPMS	0.49	0.43	NA*	TF; also binds to RNA; coactivator of transcription
ABCF2	0.49	0.54	0.60	unknown functions
PLXDC2	0.49	0.60	NA*	contains a plexin domain; unknown functions
JUP	0.49	0.48	0.53	component of junctional plaques
HIC2	0.49	0.60	0.64	unknown functions
SARS2	0.50	0.74	NA*	Ser-tRNA ligase, mitochondrial
TGDS	0.50	0.50	0.59	dTDP-D-glucose-4,6-dehydratase
CTU1	0.50	0.72	NA*	thiolation of mcm5S(2)U at tRNA wobble positions
CDK5	0.50	0.55	0.49	cyclin-dependent-like kinase 5
ALDH1L2	0.50	0.59	NA*	10-formyltetrahydrofolate dehydrogenase
DLC1	0.50	0.42	NA*	a Rho GTPase-activating protein
UPP1	0.50	0.39	NA*	uridine phosphorylase
HOXB9	0.50	0.39	0.67	TF; roles in forming the anterior-posterior axis

Fig. S13*D*. *Continuation of Fig.* S13*A*-*C*. Quantitative MS analyses, using the TMT-SPS-MS3 method (10). Human proteins whose relative levels were decreased (from <0.47-fold to 0.50-fold) in 2-KO [*hsUBR1*$^{-/-}$ *hsUBR2*$^{-/-}$] HEK293T cells (2-KO cell line #1 and 2-KO cell line #2) vs. wild-type HEK292T cells are cited in the second and third columns, respectively. The entries are cited in the order of fold-values determined for 2-KO cell line #1 vs. wild-type HEK293T cells. Fold-values for the corresponding mRNAs, determined by RNA-seq (with RNA from 2-KO cell line #1 vs. RNA from wild-type cells) are cited in the fourth column. NA* ("not applicable") refers to the absence of detectable mRNA levels in both 2-KO and wild-type cell lines. In the fifth column, transcription factors (TFs) and components of the ubiquitin-proteasome system are in red and blue, respectively. Functions of the cited proteins were compiled using entries in Uniprot (https://www.uniprot.org/) and/or GeneCards (https://www.genecards.org/). See also Fig. 2 and *SI Appendix*, Materials and Methods.

SI Materials and Methods

Antibodies, Cell Media, and Other Reagents

The following primary antibodies were used for immunoblotting (IB): anti-flag M2 mouse monoclonal antibody (Sigma, F1804); anti-ha rabbit polyclonal antibody (Sigma, H6908); anti-GAPDH 6C5 mouse monoclonal antibody to human/mouse glyceraldehyde 3-phosphate dehydrogenase (Santa Cruz, SC-32233); anti-*hs*ADRB2 rabbit polyclonal antibody (Proteintech, 13096-1-AP); anti-*hs*DACH1 rabbit polyclonal antibody (Proteintech, 10914-1-AP); anti-GR D8H2 mouse monoclonal antibody to human glucocorticoid receptor (Cell Signaling, 3660); anti-NF-L (NFEL) C28E10 rabbit monoclonal antibody to human neurofilament light subunit (Cell Signaling, 2837); anti-NF-M (NFEM) 2H3 mouse monoclonal antibody to human neurofilament medium subunit (DSHB); anti-*hs*UBR1 A-5 mouse monoclonal antibody (Santa Cruz, SC-515753); and anti-*hs*UBR2 rabbit polyclonal antibody (Bethyl, A305-416-A). Anti-*hs*UBR1 and anti-*hs*UBR2 also recognized *mm*UBR1 and *mm*UBR2, respectively. Secondary antibodies for IB were goat anti-mouse IRDye 800CW conjugate (Li-Cor, C60405-05); goat anti-mouse HRP conjugate (Bio-Rad, 1706516); and goat anti-rabbit HRP conjugate (Bio-Rad, 1706515). Proteins on IB membranes were detected and quantified using Odyssey-9120 near-infrared imaging system (Li-Cor, Lincoln, NE). IB-based detection also used chemilumenescence (Amersham ECL Prime Western Blotting Detection Reagent; GE Healthcare, RPN2232).

Human cells lines were grown in DMEM containing also 4.5 g/L glucose, L-glutamine, sodium pyruvate (Corning, 10-013-CV). Growth media were supplemented with GlutaMAX (Gibco, 35050061) and penicillin-streptomycin (Genesee Scientific, 25-512). For propagation of cell cultures, cell monolayers were treated with trypsin-EDTA (VWR, 0154-0100). Transfections were carried out using GeneJuice Transfection Reagent (Sigma, 70967) and the manufacturer's protocol. "Complete protease inhibitor cocktail" (Roche, 11697498001) was added to lysis buffers for preparation of cell extracts. SDS-PAGE was carried out using 8%, 10%, 12%, or 4-12% NuPAGE Bis-Tris Gels (ThermoFisher. Other reagents were restriction endonucleases, T4 DNA ligase, and Q5 DNA polymerase (New England Biolabs).

RNA-seq Analyses of Wild-Type Versus 2-KO [*hsUBR1*$^{-/-}$ *hsUBR2*$^{-/-}$] Human HEK293T Cell Lines

RNA-seq was carried out with RNA preparations from wild-type vs. 2-KO [*UBR1*$^{-/-}$ *UBR2*$^{-/-}$] human HEK293T cell lines using standard methods(2, 3) (Fig. 2 and *SI Appendix*, Figs. S2-S7). The wild-type (parental) HEK293T cell line (American Type Culture Collection, https://www.atcc.org/products/all/crl-3216.aspx) (13) was maintained as described (1). 2-KO HEK293T cell lines were constructed and characterized as described previously (1) (see also Fig. 2A), using the parental cell line (13) and sequential knockouts of *hsUBR1* and *hsUBR2* by the CRISPR-Cas9 technique (14-16).

500,000 cells of wild-type and 2-KO [*UBR1*$^{-/-}$ *UBR2*$^{-/-}$] HEK293T cell lines were seeded, in triplicates, onto 10-cm plates, and cultures were incubated for 15 hrs at 37°C. Cell monolayers were gently washed once with phosphate-buffered saline (PBS) at room temperature (RT), then treated with 0.25% trypsin-EDTA (VWR, L0154-0100), and cell suspensions were passed through 40 μm nylon mesh filters (Bioland, CS040-01). ~1,000,000 cells of each sample were used to isolate and purify RNA. RNA-seq analyses were performed with three independently prepared RNA samples from cells of wild-type and 2-KO genotypes. Cells were lysed using

QIAshredder (QIAGEN 79654). RNA were purified using RNAeasy Mini Kit (QIAGEN 74104). RNA samples were treated with RNase-Free DNase (QIAGEN 79254). mRNA preparations were obtained using NEBNext Poly(A) Magnetic Isolation Module (NEB E7490). cDNA libraries were produced from resulting mRNA preparations using NEBNext Ultra II Library Prep Kit (NEB E7770). Sequencing of cDNA libraries was carried out using Illumina HiSeq2500 System (2, 3).

The resulting (output) FASTQ files were analyzed using Galaxy server (https://usegalaxy.org/) (17). Quality of FASTQ files was assessed using FastQC (http://www.bioinformatics.babraham.ac.uk/projects/fastqc). Alignments to the latest human reference genome GRCh38 (18) were carried out using Bowtie2 (19) resulting in BAM alignment files (20). Alignments were visualized using BAM files and the UCSC Genome Browser (http://genome.ucsc.edu/)(21). Alignment reads were quantified using BAM files and FeatureCounts (22). DESeq2 (23) and R (https://www.R-project.org/) were used to analyze the observed changes in measured levels of specific RNAs (see also Results). Genes were annotated using org.Hs.eg.db (24).

The levels of specific mRNAs in cells of a given genotype, used to calculate the ratios (fold-values), were the averages of RNA-seq measurements with three independently prepared RNA samples from wild-type and 2-KO [*UBR1*$^{-/-}$ *UBR2*$^{-/-}$] HEK203T cells, respectively. The scatter of RNA-seq data among three datasets for two cell lines (particularly for mRNAs whose levels changed by more than 2-fold in either direction) was quite low, <5% (*SI Appendix*, Fig. S2). The levels of some RNA-seq-quantified mRNAs, particularly the ones strongly increased or decreased in 2-KO vs. wild-type HEK293T cells, were also measured, independently, by two other methods, ^{32}P-Northern hybridizations and/or reverse transcription-quantitative PCR (RT-qPCR) (Fig. 2 and *SI Appendix*, Figs. S2-S7). In these measurements, a second, independently constructed 2-KO HEK293T cell line (denoted as 2-KO #2) was used as an additional control (Fig. 2*B*, *E* and *SI Appendix*, Fig. S3).

Mass Spectrometric (TMT-SPS-MS3) Analyses of Proteins in Wild-Type Versus 2-KO [*hsUBR1*$^{-/-}$ *hsUBR2*$^{-/-}$] Human HEK293T Cell Lines

These MS-based analyses employed the TMT-SPS-MS3 method (10) (SI Appendix, Fig. S11) and were performed using protein preparations from the above-described wild-type vs. 2-KO HEK293T cells. ~500,000 cells of wild-type and 2-KO HEK293T cell line clones were seeded, in triplicates, onto 10-cm plates, and cultures were incubated for 15 hr at 37°C. Cell monolayers were gently washed once with phosphate-buffered saline (PBS) at room temperature (RT), then treated with 0.25% trypsin-EDTA (VWR, L0154-0100), and cell suspensions were passed through 40 μm nylon mesh filters (Bioland, CS040-01). Each sample was split in half and flash frozen in liquid N_2. One half of each sample was used for IB analyses using anti-*hs*UBR1 and anti-*hs*UBR2 antibodies, to verify the 2-KO state of [*UBR1*$^{-/-}$ *UBR2*$^{-/-}$] HEK293T cells (*SI Appendix*, Fig. S10). The other half was used for TMT-SPS-MS3 analyses.

MS sample processing. Cell pellets were lysed using 8 M urea in 0.2 M EPPS buffer (pH 8.5) supplemented with protease inhibitors (Roche, 11697498001). DNA was sheared by 20 passages through a 20g syringe. Protein concentration was determined using a BCA assay. 100 μg of total protein was used for each Tandem Mass Tag (TMT; Thermo-Fisher, A34808) channel. Protein extracts were reduced with 5 mM (final concentration) TCEP (tris(2-carboxyethyl)phosphine) for 30 min, alkylated with 10 mM (final concentration) iodoacetamide for 30 min in the dark, then quenched with 10 mM (final concentration) DTT (dithiothreitol) for

15 min. All steps were performed at room temperature (RT). Proteins were then precipitated with chloroform/methanol. Briefly, to 0.1 ml of each sample, 0.4 ml of methanol was added, followed by 0.1 ml of chloroform, with thorough vortexing. Next, 0.3 ml of HPLC-grade water was added, and samples were vortexed thoroughly. Each sample was centrifuged at 14,000*g* for 5 min at RT. Both aqueous and organic layers were removed. A protein pellet was washed twice with methanol (1 ml) and centrifuged at 14,000*g* for 5 min at RT. Washed protein pellets were re-solubilized in 0.1 ml of 0.2 M EPPS buffer (pH 8.5) and proteins were digested overnight with Lys-C (enzyme/protein ratio of 1:100) at RT. Next day, MS-grade trypsin (1:100 ratio) (Pierce, #90058) was added, followed by incubation at 37°C for 6 hr.

To each digested sample, 30 µl of anhydrous acetonitrile (ACN) was added, and peptides were labeled using 0.2 mg of TMT 10-plex reagents (1 hr at RT). Excess of TMT reagent was quenched with 0.5% hydroxylamine. To equalize protein loading, a ratio check was performed by pooling 1 µl (~1 µg) of each TMT-labeled sample. Samples were pooled and desalted using in-house packed Empore C18 (3M) StageTips and analyzed by LC-MS/MS. Based on the ratio check, samples were mixed 1:1 across all TMT channels and desalted using a 100 mg Sep-Pak solid phase extraction cartridge (Waters). Desalted peptides were fractionated by basic-pH reverse-phase (bRP) HPLC using an Agilent 300 extend C18 column and collected into a 96 well plate. Samples were consolidated into 24 fractions, and 12 nonadjacent fractions were desalted using StageTips prior to analyses using LC-MS/MS.

MS data acquisition. TMT-labeled peptides were resuspended in 5% ACN/5% formic acid and loaded onto an in-house pulled C18 column (30cm, 2.6 µm Accucore (Thermo-Fisher, 100 µm internal diameter) with 100% buffer A (5% ACN, 0.125% formic acid) and eluted using a 90-min linear gradient from 0% to 30% buffer B (95% ACN, 0.125% formic acid). Eluted peptides were injected into an Orbitrap Fusion mass spectrometer equipped with a Thermo FAIMS Pro device, which was run using default parameters (25, 26) Briefly, FAIMS inner and outer electrodes were set to 100C, with transport gas preset to 4.7 L/min. Three FAIMS compensation voltages (40, 60, 80) were used during acquisition. Peptides were acquired using synchronous precursor selection (SPS-MS3) method (27) for TMT quantification. Briefly, high resolution MS1 precursor scans were acquired at 120 K resolution, 1e5 AGC target with a maximum of 50 ms injection time. MS2 spectra were acquired by selecting the top ten most abundant features via collisional induced dissociation (CID) of 35% in the ion trap, 2e4 AGC target, quadrupole isolation width of 0.7 *m*/*z* and a maximum ion time of 50 ms. For MS3 acquisition, a synchronous precursor selection of ten fragment ions was acquired with an AGC of 2e5 K for 100 ms and a HCD collision energy of 65%.

MS data analysis. All acquired raw data were converted to mzXML. Spectra were searched with Comet (28), using an in-house proteomic pipeline against the human Uniprot database (February 2014), appended with reverse protein sequences and common contaminants. Searches were completed with the following parameters: 50 ppm precursor tolerance, fragment ion tolerance of 0.9 Da, static modifications of TMT (+229.163 Da) on lysine and peptide N-termini, and carbamidomethylation of cysteine residues (+57.021 Da), while oxidation of methionine residues (+15.995 Da) was set as a variable modification, and two missed cleavages were allowed. Briefly, peptide spectral libraries were first filtered to a peptide false discovery rate (FDR) of less than 1% using linear discriminant analysis (29) employing a target decoy strategy (30) The resulting peptides were further filtered to obtain a <1% protein FDR using the picked FDR method (31) Reporter ion intensities were adjusted to correct for impurities during synthesis of TMT reagents according to the manufacturer's specifications. For quantitation, a

total sum signal-to-noise of all report ions of 100 was required for analysis, isolation specificity >0.50. Protein quantitative values were normalized (column normalization) so that the sum of the signal for all protein in each channel was equal to account for sample loading.

Cell Viability and Proliferation Assays

Cell viability and proliferation were assayed using Trypan Blue exclusion test (32). Wild-type and 2-KO HEK293T cells were seeded, in quadruplicate for each genotype, at 500 cells/well in 24-well plates in DMEM-based medium described above, and were grown at 37°C. At indicated time points, cell monolayers were gently washed PBS at 37°C, then treated with 0.25% trypsin-EDTA (VWR, L0154-0100). Trypsin was inactivated by adding one volume of DMEM-based medium. Trypan blue dye (Gibco, 15250061) was added to cell suspensions at 0.2% (v/v). Cells were immediately counted using a hemocytometer under the microscope.

Cell Toxicity Assays with Methyloxalylglycine (MOG), Which Is Imported by the *hs*MCT2 Transporter

N-oxalylglycine (NOG), an analog of α-ketoglutarate (αKG), is a cytotoxic inhibitor of αKG-dependent dioxygenases (αKGDDs), but it cannot efficaciously enter mammalian cells (33). Dimethyloxalylglycine (DMOG), a derivative of NOG, is rapidly hydrolyzed, in aqueous solutions, to methyloxalylglycine (MOG) (33). The latter is converted to NOG upon MOG's entry into cells. The import of MOG has been shown to be mediated largely by the MCT2 (SLC16A7) transporter (33). Consequently, a higher level of *hs*MCT2 in 2-KO HEK293T cells, in comparison to wild-type cells, would be predicted to make the former cells hypersensitive to extracellular DMOG. Other biochemical aspects of this assay are described in Results.

To compare sensitivities of 2-KO and wild-type HEK293T human cells to N-oxalylglycine (NOG), whose precursor MOG is imported largely by *hs*MCT2, a cell mass accumulation assay was used (33). Cells were grown in DMEM containing also 10% fetal bovine serum (FBS), 4.5 g/L glucose, L-glutamine, sodium pyruvate (Corning, 10-013-CV), GlutaMAX (Gibco, 35050061) and penicillin-streptomycin (Genesee Scientific, 25-512). Wild-type and 2-KO HEK293T cells were seeded in triplicate (for each genotype) at 25,000 cells/well in 12-well plates in the DMEM-based medium described above, and were grown at 37°C for 12 hrs. Thereafter cell monolayers were gently washed with PBS at 37°C, followed by the addition of fresh DMEM-based medium at 37°C. At the same time, either MOG (to the final concentration of 5 mM) or buffer alone were added, respectively, to experimental and control samples, followed by a further incubation for 96 hrs. Cell monolayers were then gently washed twice with ice-cold PBS (0.5 ml/well), and thereafter treated with 3.7% formaldehyde in PBS (pH 7.5) (0.5 ml/well) for 10 min at RT. Fixed cells, in each well, were gently washed with 0.5 ml/well PBS at RT, and cells were then stained with 0.1% (w/v) crystal violet solution in 20% ethanol (0.5 ml/well) at RT for 15 min. Cell monolayers were then washed twice with 0.5 ml/well water for 10 min, and air-dried. To quantify the relative amounts of cell mass per well, the dye was extracted by adding, to each well, 0.25 ml of 10% (v/v) CH_3COOH, incubating the plate, with gentle rocking, for 10 min at RT, followed by measurements of A_{600} in extracts (33).

Immunoblotting

IB analyses were carried out largely as described previously (3, 34-36). Briefly, following SDS-PAGE, fractionated proteins in a polyacrylamide gel were electroblotted onto a nitrocellulose or PVDF membrane using iBlot (Invitrogen, 25-0912; Program 3; 7-min transfer

for regular detection, or 8-min transfer for detection of high molecular mass proteins). Membranes with electroblotted proteins were blocked (3) and thereafter incubated with a relevant primary antibody, followed by either LI-COR IRDye-conjugated secondary antibodies or HRP-conjugated secondary antibodies. Protein bands were detected and quantified using Odyssey-9120 and its software, or using chemilumenescence and the ImageJ program (37).

Chase-Degradation Assays

They were carried out largely as previously described (34, 35). Briefly, wild-type and mutant HEK293T cells were seeded at 400,000 cells/well in 6-well plates in a DMEM-based medium described above, and were grown at 37°C for 2 days. Thereafter cell monolayers were gently washed with phosphate-buffered saline (PBS) at 37°C, followed by addition of fresh DMEM-based medium at 37°C. At that point, cells in "zero-time" plates were removed and processed as described below. At the same time, cycloheximide (CHX) (Sigma, C7698) was added to other wells (to the final concentration of 0.25 mg/ml), initiating the chase. For chase assays with geldanamycin (GA) treatment, geldanamycin (LC Laboratories, G-4500) was added (to the final concentration of 10 μM) together with CHX. At indicated times, cells in individual wells were briefly and gently washed with ice-cold PBS, harvested into 1.5 ml tubes, and pelleted by centrifugation at 10,000*g* for 1 min. Cells were then lysed by sonicating a suspension for 10 sec in 0.2 ml of RIPA buffer (3) containing "protease inhibitor cocktail" (Roche, 11697498001), using microtip (Branson sonicator, 101-148-062) at 10% duty cycle and output 2, followed by centrifugation at 10,000*g* for 10 min. Total protein concentration in supernatants were measured by the bicinchoninic acid (BCA) assay (ThermoFisher, 23225). The resulting samples (30 μg of total protein in 45 μl of lithium dodecyl sulfate (LDS) sample buffer) were heated at 70°C for 10 min, followed by SDS-PAGE and IB assays. Quantification of protein degradation in these assays was done using the ImageJ program (37). Briefly, ImageJ quantified the brightness of specific IB-detected protein bands vs. background brightness.

^{32}P-Northern Hybridization Analyses

^{32}P-Northerns were performed using RNA preparations from wild-type and 2-KO HEK293T cells. Cells of each genotype were seeded onto 10-cm plates, at ~500,000 cells per plate, and cultures were incubated for 15 hrs at 37°C. Cell monolayers were gently washed once PBS at room temperature (RT), then treated with 0.25% trypsin-EDTA (VWR, L0154-0100), and cell suspensions were passed through 40 μm nylon mesh filters (Bioland, CS040-01). ~1,000,000 cells of each sample were lysed using QIAshredder (QIAGEN 79654). RNA were purified using RNAeasy Mini Kit (QIAGEN 74104). RNA samples were treated with RNase-Free DNase (QIAGEN 79254). RNA was fractionated in 1% agarose RNA-denaturing gels (ThermoFisher, AM8676) and transferred onto Nytran SuperCharge nylon membranes overnight, using TurboBlotter Kit (Cytiva, 10416300) and 20xSSC buffer (3M NaCl, 0.3 M sodium citrate, pH 7.0). Nylon membranes were washed once with 2xSSC buffer and dried in an oven for 7 hrs at 80°C. Membranes (8 x 11 cm) were then pre-hybridized with 10 ml of ULTRAhyb Ultrasensitive Hybridization Buffer (ThermoFisher, AM8670).

DNA segments for producing radiolabelled RNA probes were cloned into pcDNA3 vector, with a T7 promoter upstream of cDNA sequences of human *hsADRB2* (pTV602), *hsMAGEA6* (pTV599), and *hsGAPDH* (pTV598) mRNAs. Plasmids (50 μg of each) were digested overnight with *Nde*I and *Eco*RI, and DNA fragments (which contained the T7 transcriptional promoter and a specific cDNA were purified using 1% agarose gel electrophoresis

and Zymoclean Gel DNA Recovery Kit (Zymo Research, D4008), with elution into 6 µl of water. RNA probes were produced using 20 µl reaction samples containing MAXiscript T7 Transcription Kit (ThermoFisher, AM1312) 12.5 µM [α-^{32}P] UTP (10 mCi/ml; PerkinElmer, BLU007X250UC, and 6 µg of purified DNA template. DNA was removed by treating completed reactions with 1 µl of TURBO DNase I (ThermoFisher, AM1907) for 30 min at 37°C. Radiolabelled RNA probes were purified using NucAway Spin Columns (ThermoFisher, AM10070). ^{32}P of RNA probes was measured using Beckman Coulter LS6500 liquid scintillation counter. An RNA probe (5,000,000-8,000,000 dpm) was hybridized to DNA on nylon membranes overnight in 10 ml of the above hybridization buffer. Membranes were washed twice with 10 ml of low-stringency washing buffer (ThermoFisher, AM8673) for 5 min at 68°C, and then twice with 10 ml of high-stringency washing buffer (ThermoFisher, AM8674) for 15 min at 68°C. Radioautographic exposures of membranes and quantifications were carried out using Typhoon FLA 9500 (GE Healthcare Life Sciences). For re-probing a membrane, it was incubated in 50 ml of boiling 0.1% SDS for 15 min.

Quantitative Reverse Transcription PCR (RT-qPCR)

RT-qPCR was carried out largely as described previously (38). Briefly, samples of a mouse tissue or cells grown in culture were lysed using QIAshredder (Qiagen, 79654), and RNA was purified using RNeasy Mini Kit (Qiagen, 74104), with an additional treatment by RNase-Free DNase (Qiagen, 79254) to preclude DNA contamination. RNA integrity and purity were assessed in part by spectrophotometric measurements (with $A_{260}/A_{280} > 1.8$ and $A_{260}/A_{230} > 1.5$), using NanoPhotometer (Implen), and also by agarose gel electrophoresis. Reverse transcription, to synthesize cDNA, was carried at 42°C for 1 hr in a 20 µl reaction sample containing RNA (25 ng/µl), 400 units of M-MulV Reverse Transcriptase (Lucigen, 97065-184), 20 units of RNAse Inhibitor (Lucigen, 97065-224), 6 µM Random Primer Mix (NEB, S1330S), and 2 mM Deoxynucleotide (dNTP) Solution Mix (NEB, N00447S). cDNA synthesis was terminated by heating samples at 85°C for 1 min. qPCR was carried out with 0.5 ng/µl of cDNA, 1X SYBR Green I-based qPCR Master Mix (Bioland, QP01), and 250 nM of a cDNA-specific oligonucleotide (cited in Table S2) in a 20 µl reaction sample using Mastercycler RealPlex2 (Eppendorf) and the following qPCR program: 1 cycle at 95°C for 10 min; 45 cycles at 95°C for 15 sec and at 60°C for 30 sec; 1 cycle at 95°C for 15 sec and at 60°C for 15 sec. PCR products were then subjected to increases of temperature from 60°C to 95°C at 1.75°C/min, and thereafter incubated at 95°C for 15 sec (for melting-curve analyses). All RT-qPCR assays were carried out at least in duplicate. Analyses of relative levels of gene expression were carried out using the 2-Δ/ΔCt method for a gene of interest vs. expression of the *GAPDH* gene, as previously described (39, 40).

Yeast Strains, Media, and Genetic Techniques

S. cerevisiae media included YPD (1% yeast extract, 2% peptone, 2% glucose; only most relevant components are cited); SD medium (0.17% yeast nitrogen base, 0.5% ammonium sulfate, 2% glucose)); and synthetic complete (SC) medium (0.17% yeast nitrogen base, 0.5% ammonium sulfate, 2% glucose) plus a drop-out mixture of compounds required by specific auxotrophic strains. *S. cerevisiae* strains used in this work are cited in the next section. Standard techniques were used for construction of specific *S. cerevisiae* strains and transformation by DNA (3, 41).

Split-Ubiquitin Assays

The assay's concept (42, 43) is described in Results (Fig. 4*A*). A version of split-Ub assay was carried out in *S. cerevisiae* largely as described previously (36, 44). *S. cerevisiae* NMY51 (*MAT***a** *trp1 leu2 his3 ade2 LYS2::lexA-HIS3 ade2::lexA-ADE2 URA3::lexA-lacZ*) (Dualsystems Biotech AG, Schlieren, Switzerland) was cotransformed with split-Ub-based bait and prey plasmids (Table S1) using the lithium acetate method (41). Transformants were selected for the presence of both bait and prey plasmids during ~3 days of growth at 30°C on SC(-Trp, -Leu) medium (minimal medium containing 2% glucose, 0.67% yeast nitrogen base, 2% bacto-agar, and complete amino acid mixture that lacked Leu and Trp). Single colonies of resulting cotransformants were grown in SC(-Trp, -Leu) liquid medium to A_{600} of ~1.0, a near-stationary phase. The cultures were thereafter serially diluted by 3-fold, and 10 µl samples of cell suspensions were spotted onto either double-dropout SC(-Trp, -Leu), triple-dropout SC(-Trp,-Leu,-His) plates, or quadruple-dropout SC(-Trp,-Leu,-His,-Ade), which were incubated at 30°C for 2 to 4 days.

Table S1. Plasmids used in this study.

Name	Description	Source
pDHB1	Split-Ub vector, Ost4-C_{Ub}-LexA-VP16	MoBiTec, P01001DS
pPR3-N	Split-Ub vector, N_{UbG} vector	MoBiTec, P01001DS
pTV471	Ost4-C_{Ub}-*hs*UBR1-LexA-VP16	This study
pTV472	Ost4-C_{Ub}-*hs*UBR1$^{1-1059}$-LexA-VP16	This study
pTV473	Ost4-C_{Ub}-*hs*UBR1$^{1060-1749}$-LexA-VP16	This study
pTV469	N_{UbG}-*hs*PREP1	This study
pTV620	N_{UbG}-*hs*GR-A	This study
pTV621	N_{UbG}-*hs*GR-D	This study
pTV598	pcDNA3 based plasmid for generating RNA probe against *hsGAPDH*	This study
pTV599	pcDNA3 based plasmid for generating RNA probe against *hsMAGEA6*	This study
pTV602	pcDNA3 based plasmid for generating RNA probe against *hsADRB2*	This study

Table S2. Oligonucleotide primers used in this study.

Name	Nucleotide Sequence (5'-3')	Use
TV1029	AAGCTTGGTACCCAGGAAATGAGCTTGACA	Cloning pTV598
TV1030	TCTGCAGAATTCGTTTACATGTTCCAATAT	Cloning pTV598
TV1031	AAGCTTGGTACCTCACTCTTCCCCCTCTCT	Cloning pTV599
TV1032	AAGCTTGGTACCTTAAATGTTAGTTTCTCT	Cloning pTV599
TV1035	AAGCTTGGTACCCAGCAGTGAGTCATTTGT	Cloning pTV602
TV1036	TCTGCAGAATTCATGTCCAGAACCTTAGCC	Cloning pTV602
TV1015	ATGATGCGGGTTTCCAATCG	RT-qPCR for hsB4GALT6
TV1016	GATATGTGTTGGCGATGCCT	RT-qPCR for hsB4GALT6
TV1019	CCACGCCGGACAGAATAGAT	RT-qPCR for hsBARX1
TV1020	CTGGTACCACGTCTTCACCT	RT-qPCR for hsBARX1
TV987	TCCTGCTTATCCTTGTGCTGA	RT-qPCR for hsCDH2
TV988	GTTTGGCCTGGCGTTCTTTA	RT-qPCR for hsCDH2
TV997	AGAAGACCTCTGCACTGACC	RT-qPCR for hsCELSR3
TV998	AAGGCTAGGATGCTGTGGTT	RT-qPCR for hsCELSR3
TV985	TCTACTGTACGCGCTACTCG	RT-qPCR for hsEN2
TV986	CGCTTGTCCTCTTTGTTCGG	RT-qPCR for hsEN2
TV1003	GGCCTACACACAGGTCATCT	RT-qPCR for hsGAA
TV1004	GGTCACACGTACCAGCTCAT	RT-qPCR for hsGAA

TV724	CTCCTCCTGTTCGACAGTCA	RT-qPCR for hsGAPDH
TV725	CGACCAAATCCGTTGACTCC	RT-qPCR for hsGAPDH
TV1000	TCCAGCAGTTTCCTGTAAGC	RT-qPCR for hsINA
TV999	ACACCAAGAGTGAGATGGCA	RT-qPCR for hsINA
TV1017	TCAGGGACCTTCTCAGGTACT	RT-qPCR for hsLGALS3BP
TV1018	GCTTGTGGAAGCACTTGACT	RT-qPCR for hsLGALS3BP
TV991	AGCTGGTGACCATGTCTGTG	RT-qPCR for hsMAF
TV992	ATCACCTCCTCCTTGCTGAC	RT-qPCR for hsMAF
TV975	CCAAGGGCCCTCATTGAAAC	RT-qPCR for hsMAGEA6
TV976	CTCTCAAAGCCCACTCATGC	RT-qPCR for hsMAGEA6
TV1005	CTTGCAAGCCAGACTCAAGG	RT-qPCR for hsMBNL3
TV1006	AGTTGCAGTGTACCAGGCT	RT-qPCR for hsMBNL3
TV1007	CGCCGCCAAGACATATGAG	RT-qPCR for hsMSX2
TV1008	GAGGAGCTGGGATGTGGTAA	RT-qPCR for hsMSX2
TV1021	CCTGCAGAGCAAGGAATGTG	RT-qPCR for hsMYD88
TV1022	TTGGTGTAGTCGCAGACAGT	RT-qPCR for hsMYD88
TV995	TCAATGACAAGGTGGCCAAG	RT-qPCR for hsNPTX1
TV996	GTGGTCCAGGTGACACAGAT	RT-qPCR for hsNPTX1
TV1013	TGGAACCCTGATCTCACACC	RT-qPCR for hsPCDH9

TV1014	CCAAAGGCCCATCAGAGTTG	RT-qPCR for hsPCDH9
TV979	AGACAGCAGCAAGGTGTGTA	RT-qPCR for hsRNF125
TV980	AACGGCAAAGTGGACAGAAC	RT-qPCR for hsRNF125
TV981	ACGGGCCTTAGACCTTGAAA	RT-qPCR for hsRNF138
TV982	TCACTCCTATTGCTGTTCCCT	RT-qPCR for hsRNF138
TV1009	GTGTGGCCCAGTTCTTCTTG	RT-qPCR for hsSLC16A7
TV1010	CGCTTGCTGCTACCACAATA	RT-qPCR for hsSLC16A7
TV1025	CCTTTGGCACTCTCAACCAG	RT-qPCR for hsSLC2A3
TV1026	GCTCTTCAGACCCAAGGATG	RT-qPCR for hsSLC2A3
TV977	CATGAGAGCTGTGTGCTGTC	RT-qPCR for hsTLE4
TV978	AGGTGTTCTCCAGGCATTCA	RT-qPCR for hsTLE4
TV1001	CCTGGTGGAGCATAAGACCT	RT-qPCR for hsTRIM25
TV1002	TTTGCAGTCATCCGCACATC	RT-qPCR for hsTRIM25
TV983	TGAGCTTGATGCTGTGGAGA	RT-qPCR for hsZNF24
TV984	ACCATCATCATCACAGTGCCT	RT-qPCR for hsZNF24

SI References

1. Vu TTM, Varshavsky A (2020) The ATF3 transcription factor is a short-lived substrate of the Arg/N-degron pathway. *Biochemistry* 59:2796-2812.
2. Van der Berge K, *et al.* (2019) RNA sequencing data: hitchhiker's guide to expression analysis. *Annu. Rev. Biomed. Data Sci.* 2:139-173.
3. Ausubel FM, *et al.* (2017) *Current Protocols in Molecular Biology.* (Wiley-Interscience, New York).
4. Conesa A, *et al.* (2016) A survey of best practices for RNA-seq data analysis. *Genome Biol.* 17:13.
5. Bahouth SW, Beauchamp MJ, Vu KN (2002) Reciprocal regulation of beta(1)-adrenergic receptor gene transcription by Sp1 and early growth response gene 1: induction of EGR-1 inhibits the expression of the beta(1)-adrenergic receptor gene. *Mol. Pharmacol.* 61:379-390.
6. Jaeger A, Fritschka S, Ponsuksili S, Wimmers K, Murani E (2015) Identification and functional characterization of cis-regulatory elements controlling expression of the porcine ADRB2 gene. *Int. J. Biol. Sci.* 11:1006-1015.
7. Baeyens DA, McGraw DW, Jacobi SE, Cornett LE (1998) Transcription of the beta2-adrenergic receptor gene in rat liver is regulated during early postnatal development by an upstream repressor element. *J. Cell. Physiol.* 175:333-340.
8. Li L, He S, Sun JM, Davie JR (2004) Gene regulation by Sp1 and Sp3. *Biochem. Cell Biol.* 82:460-471.
9. O'Connor L, Gilmour J, Bonifer C (2016) The Role of the ubiquitously expressed transcription factor Sp1 in tissue-specific transcriptional regulation and in disease. *Yale J. Biol. Med.* 89:513-525.
10. Navarrete-Perea J, Yu Q, Gygi SP, Paulo JA (2018) Streamlined tandem mass tag (SL-TMT) protocol: an efficient strategy for quantitative (phospho)proteome profiling using tandem mass tag-synchronous precursor selection-MS3. *J. Proteome Res.* 17:2226-2236.
11. Varshavsky A (2019) On the cause of sleep: protein fragments, the concept of sentinels, and links to epilepsy. *Proceedings of the National Academy of Sciences of the United States of America* 116:10773-10782.
12. Crawford ED, *et al.* (2013) The DegraBase: a database of proteolysis in healthy and apoptotic human cells. *Mol. Cell. Proteomics* 12(3):813-824.
13. Stepanenko AA, Dmitrenko VV (2015) HEK293 in cell biology and cancer research: phenotype, karyotype, tumorigenicity, and stress-induced genome-phenotype evolution. *Gene* 569:182-190.
14. Ran FA, *et al.* (2013) Genome engineering using the CRISPR-Cas9 system. *Nat. Protoc.* 8:2281-2308.
15. Zheng Q, *et al.* (2014) Precise gene deletion and replacement using the CRISPR/Cas9 system in human cells. *BioTechniques* 57(3):115-124.
16. Knott GJ, Doudna JA (2018) CRISPR-Cas guides the future of genetic engineering. *Science* 361:866-869.
17. Afgan E, *et al.* (2018) The Galaxy platform for accessible, reproducible and collaborative biomedical analyses: 2018 update. *Nucl. Acids Res.* 46:W537–W544.

18. Schneider VA, *et al.* (2017) Evaluation of GRCh38 and de novo haploid genome assemblies demonstrates the enduring quality of the reference assembly. *Genome Res.* 27:849-864.
19. Langmead B, Salzberg SL (2012) Fast gapped-read alignment with Bowtie 2. *Nat. Methods* 9:357-359.
20. Li H, *et al.* (2009) The sequence alignment/map format and SAMtools. *Bioinformatics (Oxford, England)* 25(16):2078-2079.
21. Kent WJ, *et al.* (2002) The human genome browser at UCSC. *Genome Res.* 12: 996–1006.
22. Liao Y, Smyth GK, Shi W (2014) featureCounts: an efficient general purpose program for assigning sequence reads to genomic features. . *Bioinforma* 30:923–930.
23. Love MI, Huber W, Anders S (2014) Moderated estimation of fold change and dispersion for RNA-seq data with DESeq2. *Genome Biol.* 15:550
24. Carlson M (2019) org.Hs.eg.db: Genome wide annotation for Human. R package version 3.8.2 (DOI: 10.18129/B9.bioc.org.Hs.eg.db).
25. Schweppe DK, *et al.* (2019) Characterization and Optimization of Multiplexed Quantitative Analyses Using High-Field Asymmetric-Waveform Ion Mobility Mass Spectrometry. *Anal Chem* 91(6):4010-4016.
26. Schweppe DK, Rusin SF, Gygi SP, Paulo JA (2020) Optimized Workflow for Multiplexed Phosphorylation Analysis of TMT-Labeled Peptides Using High-Field Asymmetric Waveform Ion Mobility Spectrometry. *J Proteome Res* 19(1):554-560.
27. McAlister GC, *et al.* (2014) MultiNotch MS3 enables accurate, sensitive, and multiplexed detection of differential expression across cancer cell line proteomes. *Anal Chem* 86(14):7150-7158.
28. Eng JK, Jahan TA, Hoopmann MR (2013) Comet: an open-source MS/MS sequence database search tool. *Proteomics* 13(1):22-24.
29. Huttlin EL, *et al.* (2010) A tissue-specific atlas of mouse protein phosphorylation and expression. *Cell* 143(7):1174-1189.
30. Elias JE, Gygi SP (2007) Target-decoy search strategy for increased confidence in large-scale protein identifications by mass spectrometry. *Nat Methods* 4(3):207-214.
31. Savitski MM, Wilhelm M, Hahne H, Kuster B, Bantscheff M (2015) A Scalable Approach for Protein False Discovery Rate Estimation in Large Proteomic Data Sets. *Mol Cell Proteomics* 14(9):2394-2404.
32. Strober W (2015) Trypan Blue exclusion test of cell viability. *Curr. Protoc. Immunol.* 111:A3.b.1-a3.b.3.
33. Fets L, *et al.* (2018) MCT2 mediates concentration-dependent inhibition of glutamine metabolism by MOG. *Nat. Chem. Biol.* 14:1032-1042.
34. Wadas B, *et al.* (2016) Degradation of serotonin N-acetyltransferase, a circadian regulator, by the N-end rule pathway. *J. Biol. Chem.* 291:17178-17196.
35. Piatkov KI, Brower CS, Varshavsky A (2012) The N-end rule pathway counteracts cell death by destroying proapoptotic protein fragments. *Proc. Natl. Acad. Sci. USA* 109:E1839-E1847.
36. Oh JH, Hyun JY, Varshavsky A (2017) Control of Hsp90 chaperone and its clients by N-terminal acetylation and the N-end rule pathway. *Proc. Natl. Acad. Sci. USA* 114:E4370-E4379.

37. Schneider CA, Rasband WS, Eliceiri KW (2012) NIH Image to ImageJ: 25 years of image analysis. *Nat. Methods* 9:671-675.
38. Green MR, Sambrook J (2012) *Molecular Cloning: A Laboratory Manual (4th edition)* (Cold Spring Harbor Laboratory Press: Cold Spring Harbor, N.Y).
39. Pfaffl MW (A New Mathematical Model for Relative Quantification in Real-Time RT-PCR. *Nucl. Ac. Res.* 29:e45.
40. Livak KJ, Schmittgen TD (2001) Analysis of Relative Gene Expression Data Using Real-Time Quantitative PCR and the 2(-Delta Delta C(T)) Method. *Methods* 25 402–408.
41. Andrews B, Boone C, Davis TN, Fields S (2016) *Budding Yeast (a laboratory manual).* (Cold Spring Harbor Press, Cold Spring Harbor, NY).
42. Johnsson N, Varshavsky A (1994) Split ubiquitin as a sensor of protein interactions in vivo. *Proc. Natl. Acad. Sci. USA* 91:10340-10344.
43. Dunkler A, Muller J, Johnsson N (2012) Detecting protein-protein interactions with the split-ubiquitin sensor. *Methods Mol. Biol.* 786:115-130.
44. Gisler SM, *et al.* (2008) Monitoring protein-protein interactions between the mammalian integral membrane transporters and PDZ-interacting partners using a modified split-ubiquitin membrane yeast two-hybrid system. *Mol. Cell. Proteomics* 7:1362-1377.